Anabolic SIRT4 Exerts Retrograde Control over TORC1 Signaling by Glutamine Sparing in the Mitochondria

Eisha Shaw,[a] Manasi Talwadekar,[a] Zeenat Rashida,[b] Nitya Mohan,[a*] Aishwarya Acharya,[a*] Subhash Khatri,[a] Sunil Laxman,[b] Ullas Kolthur-Seetharam[a]

[a]Department of Biological Sciences, Tata Institute of Fundamental Research, Colaba, Mumbai, India
[b]Regulation of Cell Fate, Institute of Stem Cell Science and Regenerative Medicine (InStem), Bangalore, India

ABSTRACT Anabolic and catabolic signaling mediated via mTOR and AMPK (AMP-activated kinase) have to be intrinsically coupled to mitochondrial functions for maintaining homeostasis and mitigate cellular/organismal stress. Although glutamine is known to activate mTOR, whether and how differential mitochondrial utilization of glutamine impinges on mTOR signaling has been less explored. Mitochondrial SIRT4, which unlike other sirtuins is induced in a fed state, is known to inhibit catabolic signaling/pathways through the AMPK-PGC1α/SIRT1–peroxisome proliferator-activated receptor α (PPARα) axis and negatively regulate glutamine metabolism via the tricarboxylic acid cycle. However, physiological significance of SIRT4 functions during a fed state is still unknown. Here, we establish SIRT4 as key anabolic factor that activates TORC1 signaling and regulates lipogenesis, autophagy, and cell proliferation. Mechanistically, we demonstrate that the ability of SIRT4 to inhibit anaplerotic conversion of glutamine to α-ketoglutarate potentiates TORC1. Interestingly, we also show that mitochondrial glutamine sparing or utilization is critical for differentially regulating TORC1 under fed and fasted conditions. Moreover, we conclusively show that differential expression of SIRT4 during fed and fasted states is vital for coupling mitochondrial energetics and glutamine utilization with anabolic pathways. These significant findings also illustrate that SIRT4 integrates nutrient inputs with mitochondrial retrograde signals to maintain a balance between anabolic and catabolic pathways.

I t is intuitive that the ability to take up and utilize macronutrients for catabolic or anabolic purposes is intrinsically linked to cellular and organismal energetics. Thus, the sensing and utilization of various macronutrients in the mitochondria needs to be coupled to the activity of metabolic sensors in the cytosol such as AMPK (AMP-activated kinase) and mTOR (mammalian target of rapamycin) in order to orchestrate a balance between the metabolic state of the cell and external stimuli. AMPK, mTOR, and sirtuins (Sir2-like NAD-dependent deacylases) have been well established to play central roles in linking nutrient and energetic status to cellular and organismal physiology (1–5). While the AMPK-sirtuin (6–9) and AMPK-mTOR (10, 11) cross talks are well worked out, the relative interdependence and hierarchy of signals between these sensors is not well explored. Further, functional interactions between sirtuins and mTOR are poorly understood and are largely limited to SIRT1 (12–14).

Anaplerotic pathways are essential to maintain physiological homeostasis under carbohydrate deprivation states. Increased utilization of glutamine via α-ketoglutarate (α-KG), largely determined by the activity of glutamate dehydrogenase (GDH) within the mitochondria, is important under both normal and pathophysiological conditions,

Address correspondence to Ullas Kolthur-Seetharam, ullas@tifr.res.in.

* Present address: Nitya Mohan, Immunotherapy and Immunoprevention, German Cancer Research Center (DKFZ), Heidelberg, Germany; Aishwarya Acharya, Max Planck Institute for Biology of Aging, Cologne, Germany.

including cancer (15, 16). Interestingly, both α-KG and glutamine have been recently reported to impact TORC1 signaling (17, 18). However, under normal physiological settings, whether and how differential mitochondrial uptake and utilization of glutamine affect TORC1 is still unknown. In this context, mTOR is both activated and inhibited by α-KG (18, 19). Although glutaminolysis that generates α-KG was shown to induce mTOR in cancer cells (18), α-KG-mediated inhibition of mitochondrial ATP-synthase led to life span extension via mTOR inhibition (19). These are clearly contradictory findings, and hence further investigation is required to unravel the significance of mitochondrial glutamine utilization in regulating anabolic signaling via TORC1. Moreover, if and how mechanisms within the mitochondria that determine anaplerotic flux and energetics regulate TORC1 are questions that remain to be addressed. Specifically, it is enticing to check whether mitochondrial utilization or sparing of glutamine acts as an intracellular cue to regulate metabolic signaling.

Sirtuins are typically associated with physiological responses during fasting or calorie-restricted states (3). Intriguingly, however, SIRT4, a bona fide mitochondrial sirtuin, is induced under a fed state (20). Although reports have shown that it has ADP-ribosyltransferase (21, 22) and NAD$^+$-dependent deacylase activities (23, 24), the robust catalytic activity, as well as the biological functions, of SIRT4 is largely unknown. More importantly, although SIRT4 is established to counter catabolic signaling and negatively regulate fatty acid oxidation (20, 21, 25), whether it affects anabolic signaling remains unclear.

It should be noted that glutamate dehydrogenase (GDH) has been demonstrated to be a bona fide substrate of SIRT4 and this is critical for glutamine homeostasis (22, 26, 27). Particularly in cancers, the SIRT4/GDH/glutamine axis is known to affect cell proliferation (28), and TORC1 is known to inhibit SIRT4 expression (29). We would like to emphasize that TORC1-mediated inhibition of SIRT4 expression in cancers represents a pathophysiological state wherein there is oncogenic glutamine addiction. However, the link between SIRT4 and TORC1 under normal physiological conditions needs to be unraveled. To reiterate, in noncancerous cells, glutamine utilization by tricarboxylic acid (TCA) via the anaplerotic flux varies between a fed and a fasted state. Specifically, glycolytic pyruvate entry into the TCA is known to reduce anaplerotic utilization of glutamine during a fed state. As mentioned earlier, whether or not this links to cytosolic TOR remains an open question. Moreover, it is important to note that, unlike in cancers, both SIRT4 and TORC1 are induced under fed states (20). Hence, given that SIRT4 expression is higher in a fed state, it is enticing to investigate whether coupling of mitochondrial metabolism/energetics with mTOR is brought about by SIRT4. Further, such a hypothesis would make physiological sense since mTOR-dependent anabolic pathways, including protein synthesis and lipogenesis, are energetically demanding and aberrant activation of mTOR has been shown to cause energetic stress (30).

Here, we report that anaplerotic flux, specifically, the utilization/sparing of glutamine in the TCA cycle, constitutes a key signal mediating TORC1 activation. We further demonstrate that SIRT4 presence or absence phenocopies TORC1 signaling under a nutrient-replete or -deprived state, respectively. Thus, our study provides insights into the crucial role of SIRT4 in activating TORC1 in response to nutrients via modulation of glutamine utilization. We also demonstrate that SIRT4 enhances lipogenesis and cell proliferation and inhibits cellular autophagy. We highlight SIRT4 as an anabolic sirtuin and bring to the fore the importance of mitochondrial inputs in regulating metabolic signaling.

RESULTS

Mitochondrial glutamine sparing activates TORC1. Glutamine is a potent regulator of TORC1 activity (17, 18). However, whether altered glutamine flux under physiological conditions that mimic fed or fasted states affects mTOR signaling is still unclear. Toward this, primary hepatocytes, preincubated in amino acid- and serum-free media, were treated with 2 mM glutamine in the presence of either low (5 mM) or high (25 mM) glucose. mTOR signaling, as assessed by phosphorylation of downstream
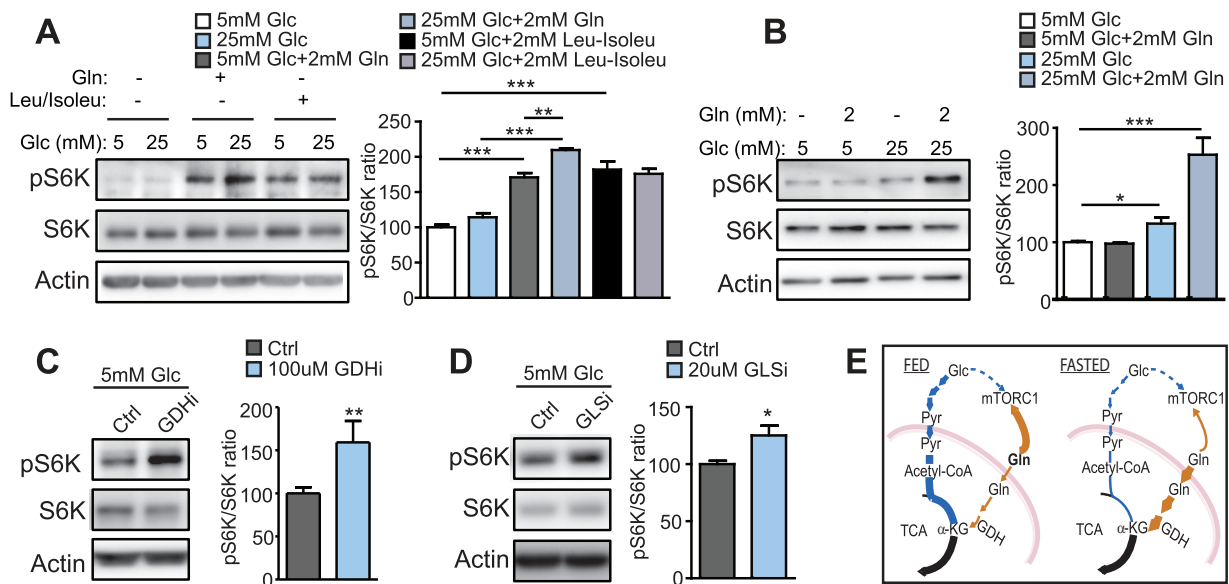
FIG 1 Glutamine sparing activates TORC1 signaling. (A to D) Immunoblots and quantitations for pS6K(Thr389)/S6K in primary hepatocytes. (A) Primary hepatocytes derived from wild-type mice, preincubated in EBSS for 3 h, followed by 1 h of incubation in low (5 mM)- and high (25 mM)-glucose (Glc)-containing EBSS with or without either 2 mM glutamine or 0.8 mM leucine/isoleucine ($n = 4$). (B) Primary hepatocytes derived from wild-type mice, under low (5 mM)- and high (25 mM)-glucose conditions with or without 2 mM glutamine (Gln) ($n = 5$). (C) Primary hepatocytes from wild-type mice treated with 100 μM EGCG (GDHi) for 1 h under 5 mM glucose ($n = 4$). (D) Primary hepatocytes from wild-type mice treated with 20 μM BPTES (GLSi) for 1 h under 5 mM glucose ($n = 4$). (E) Relative contributions of glucose (Glc) and glutamine (Gln) to the TCA cycle and mTORC1 activation under fed versus fasted states. Pyr, pyruvate; GDH, glutamate dehydrogenase; TCA, tricarboxylic acid cycle. Data represent means ± the SD (*, $P < 0.05$; **, $P < 0.001$; ***, $P < 0.0001$).

substrate S6K (pS6K), was low in glucose-alone supplemented conditions. The addition of glutamine led to a robust increase in mTOR activity, more than in the presence of leucine and isoleucine (Fig. 1A). Interestingly, glutamine-dependent activation of mTOR signaling was highest under high-glucose conditions, over and above the other treatments (Fig. 1A). In contrast to this, leucine/isoleucine activated mTOR signaling to similar extents under both low- and high-glucose conditions (Fig. 1A). Consistently, we found similar glucose-dependent glutamine-mediated increase in mTOR signaling even when hepatocytes were grown in complete media in the presence of amino acids and serum (Fig. 1B). It is intriguing that the effect of glutamine on pS6K under low-glucose conditions was still evident in the absence of serum and amino acids and indicates a possible graded response, which is dependent upon other inputs. Nevertheless, mTOR signaling was robustly induced under high-glucose conditions but not under low-glucose conditions, irrespective of serum and other amino acids mediated effects (Fig. 1A and B). Together, these suggested that glutamine effects on mTOR are potentiated in the presence of high levels of glucose. Importantly, this led us to further investigate whether differential glutamine utilization within the mitochondria, as under fed and fasted states, controls the extent of mTOR signaling.

Reduced carbohydrate availability increases anaplerotic flux of glutamine into the TCA cycle, which is regulated by the activity of glutamate dehydrogenase (GDH) (31). Thus, we surmised that inhibition of GDH, which would lower glutamine channeling into TCA, could potentiate mTOR signaling. As evident from Fig. 1C, a short-term inhibition of GDH in primary hepatocytes led to a significant increase in pS6K. It should be noted that this increase was seen even when cells were grown under low-glucose conditions, possibly due to reduced utilization of glutamine via the TCA. To confirm if this was indeed true, we also inhibited glutaminase (GLS), which converts glutamine to glutamate, which is then fed into TCA via GDH. Inhibition of GLS led to a significant increase in pS6K levels (Fig. 1D), and the effects were similar to GDH inhibition (Fig. 1C). It is important to note that activation of mTOR signaling following GDH or GLS inhibition under low-glucose conditions was comparable to glutamine supplementa-

tion under high-glucose conditions. Together, these results demonstrate that differential glutamine utilization (or sparing), under fasted and fed conditions, by the mitochondria is used as a nutrient cue to regulate mTOR signaling in the cytosol (Fig. 1E).

SIRT4 regulates TORC1 signaling. GDH activity and thus glutamine utilization in the mitochondria are known to be highly regulated during fed and fasted conditions (31). Thus, we wanted to identify the molecular factor within the mitochondria that would mediate such effects on mTOR via glutamine. Among others, mitochondrial deacylase SIRT4 has been shown to be a potent regulator of GDH activity and anaplerotic flux (21, 22). Moreover, although SIRT4 is induced under a fed state (20, 32), the functional significance of elevated SIRT4 levels in nutrient excess conditions is still unknown. Specifically, whether differential SIRT4 levels couple glutamine flux through TCA to control anabolic signaling remains to be addressed.

To investigate this, we used either SIRT4 gain-of-function (ectopic expression) or loss-of-function (knockdown or knockout) models under different metabolic states. Given that SIRT4 levels and mTOR signaling are low under fasted conditions, we assessed the effects of SIRT4 overexpression under fasted (or low-glucose) conditions. We found that ectopic expression of SIRT4 led to a robust increase in pS6K, across cell types (Fig. 2A and B). mTOR is known to exist in two complexes, *viz.*, TORC1 and TORC2, and phosphorylation of pS6K and pAKT-S473 is typically used as a bona fide indicator of signaling via either of these arms. On assessing pAKT-S473 under similar conditions, we did not find SIRT4-dependent TORC2 activation (Fig. 2C). This highlighted that SIRT4 has a specific effect on mTORC1 signaling. Rapamycin, the well-known inhibitor of mTOR, has been used to decrease signaling downstream to mTORC1, particularly at low doses (33). Consistently, we found that treating with rapamycin significantly reduced pS6K levels in both control and SIRT4-overexpressing cells (Fig. 2D). Thus, together, our data demonstrate that SIRT4 positively regulates TORC1 signaling, which is sensitive to rapamycin.

Although, TORC1 has several downstream target proteins, emerging literature indicates that phosphorylation could be highly specific based on both substrate affinities and the extent of activation (34, 35). Hence, we wanted to check whether SIRT4-dependent activation of TORC1 led to phosphorylation of 4E-BP1, a translation repressor protein, and ULK-1, which is involved in autophagy. We were surprised to find that while SIRT4-dependent TORC1 activation led to an increase in pS6K (Fig. 2A and B) and pULK1 (S757) levels (Fig. 2E), phosphorylation of 4E-BP1 was unaltered (Fig. 2F). Although this finding is intriguing, it is now well established that 4E-BP1 is a preferred substrate of TORC1 and that, whereas its phosphorylation is resistant to rapamycin treatment (33), complete starvation leads to a loss of p4E-BP1. These suggest that although minimal TORC1 activity is sufficient to phosphorylate 4E-BP1 (possibly maximally), phosphorylation of substrates like S6K is dependent on extent of mTOR activation.

Consistent with the results described above, knockdown of SIRT4 led to a significant decrease in TORC1 signaling (Fig. 2G and H). Here again, phosphorylation of 4E-BP1 remained unaltered, similar to when SIRT4 was ectopically expressed, indicating a differential effect with regard to SIRT4-dependent control of TORC1 (Fig. 2I). Importantly, TORC1 signaling was drastically reduced in primary hepatocytes from $SIRT4^{-/-}$ mice compared to the controls (Fig. 2J). Furthermore, restoring SIRT4 expression in primary hepatocytes derived from $SIRT4^{-/-}$ mice increased pS6K to levels comparable to controls, indicating the rescue of TORC1 signaling (Fig. 2J). These experiments using knockdown or knockout of SIRT4 not only ruled out the possibility of overexpression-based artifacts but also clearly established SIRT4 as a key determinant of TORC1 signaling.

Even though until now SIRT4-dependent control of TORC1 was unknown, mTOR has been previously shown to negatively regulate *Sirt4* expression. However, it should be noted that, this was shown in cancer cells (29), and it is unlikely to apply to normal physiological contexts. Importantly, SIRT4 protein levels and TORC1 signaling are
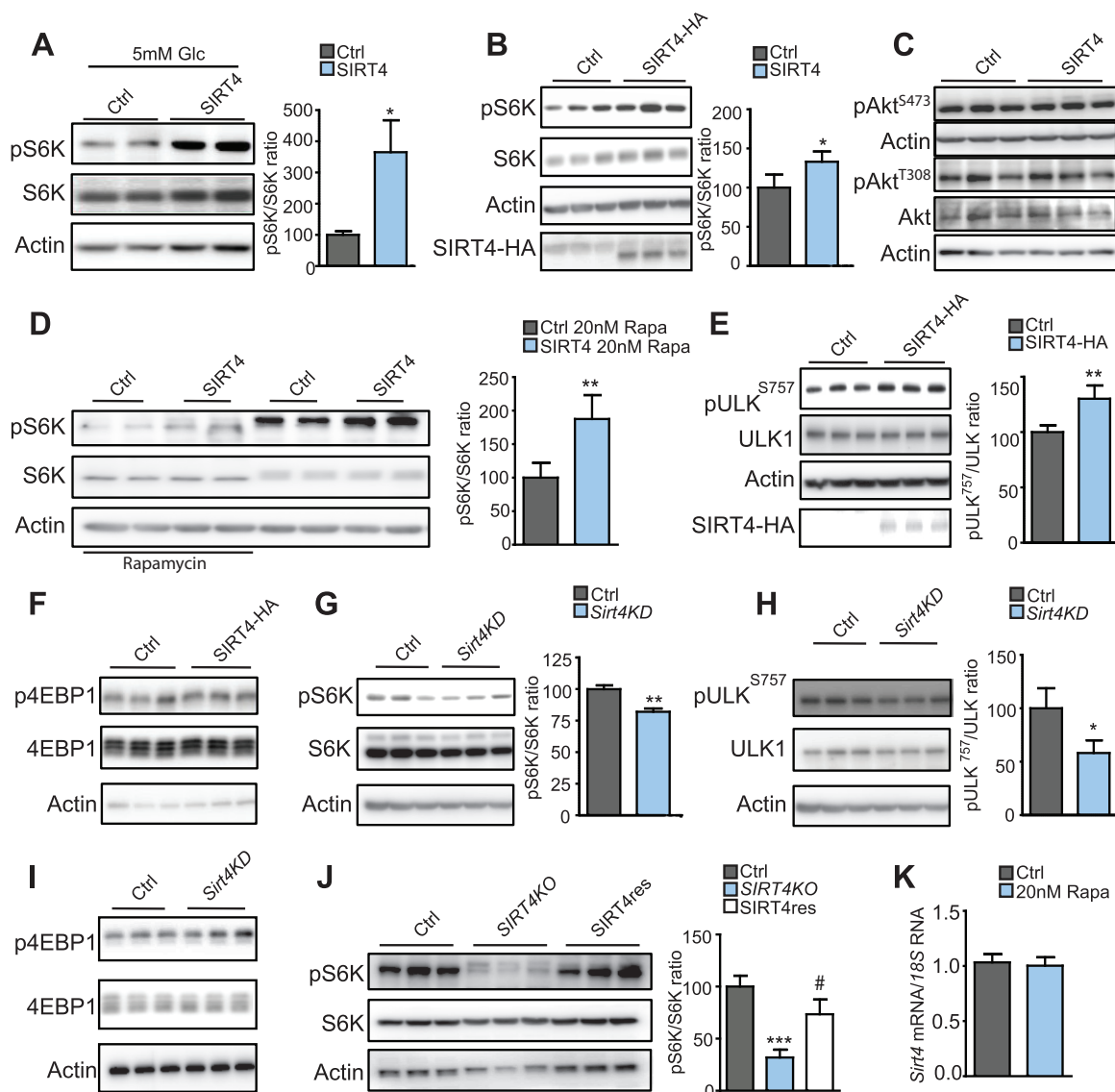
FIG 2 SIRT4 regulates mTORC1 signaling. (A and B) Immunoblots and quantitations for pS6K(Thr389)/S6K primary hepatocytes from wild-type mice adenovirally transduced with Ad-CMV (control) and Ad SIRT4 (SIRT4) under low-glucose conditions ($n = 6$) (A) and HEK293T cells transiently expressing SIRT4 and controls under low-glucose conditions ($n = 6$) (B). (C) Representative immunoblots for pAkt (Ser473), pAkt (Thr308), Akt, and actin in HEK293T cells overexpressing control or SIRT4 (SIRT4-HA) in low-glucose medium ($n = 4$). (D) Representative immunoblots for pS6K (Thr389)/S6K in primary hepatocytes adenovirally transduced with either control or SIRT4 and incubated in low-glucose medium with or without 20 nM rapamycin. (E and F) Immunoblots and quantitations for pULK757/ULK (E) and p4EBP1/4EBP1, actin, and HA (F) in control and SIRT4-HA-transfected HEK293 cells. (G to I) Immunoblots and quantitations for pS6K/S6K (G), pULK757/ULK1 (H), and p4EBP1/4EBP1 (I) in control and Sirt4 knockdown (Sirt4KD) HEK293T cells. (J) Representative immunoblots for pS6K/S6K in primary hepatocytes isolated from wild-type and SIRT4KO mice. SIRT4 expression was restored by transducing Ad-SIRT4 into SIRT4KO hepatocytes (SIRT4res) to rescue mTORC1 signaling ($n = 6$). (K) Sirt4 mRNA levels in primary hepatocytes, with and without 20 nM rapamycin treatment for 30 min, normalized to 18S ($n = 4$). The data represent means $\pm$ the SD (*, $P < 0.05$; **, $P < 0.005$; ***, $P < 0.001$; #, $P < 0.0001$).

highest under nutrient-excess or fed states across cells and tissues (2, 20, 25). Hence, given that both are induced in a fed state it is difficult to envisage a negative interaction between these factors under normal physiological conditions. Nonetheless, we wanted to check if mTOR inhibition affected *Sirt4* mRNA levels in primary hepatocytes. Unlike in cancer cells (29), we did not find *Sirt4* expression to be altered in response to rapamycin (Fig. 2K). These results clearly demonstrate that mitochondrial SIRT4 is a positive regulator of TORC1 signaling in noncancerous cells and tissues.

SIRT4 potentiates nutrient- and growth factor-dependent activation of mTORC1. Next, we wanted to explore the possibility of mitochondrial SIRT4 in poten-
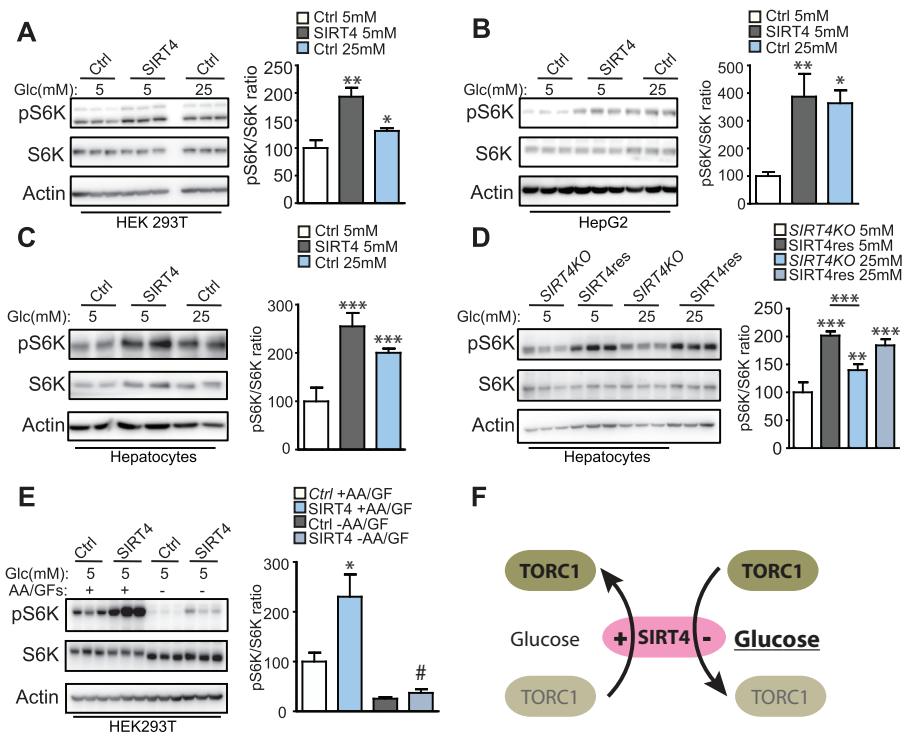
FIG 3 Sirt4 exerts control over nutrient and growth factor dependent activation of mTORC1. (A to D) Immunoblots and quantitations for pS6K/S6K and actin, as indicated, in HEK293T cells (A), HepG2 cells (B), and primary hepatocytes (C) from wild-type mice transduced with Ad-CMV (control) and Ad-SIRT4 (SIRT4) and cultured in low (5 mM)- and high (25 mM)-glucose media for 12 h ($n = 5$). (D) Primary hepatocytes isolated from SIRT4KO mice. SIRT4 expression was restored by transducing Ad-SIRT4 (SIRT4) into SIRT4KO hepatocytes (SIRT4res) and cultured in low (5 mM)- and high (25 mM)-glucose media for 12 h as depicted ($n = 6$). (E) Immunoblots for pS6K/S6K and actin, as indicated, in control and SIRT4-transfected HEK293T cells pretreated with low (5 mM)-glucose medium for 3 h (+AA/GFs), followed by 1 h of EBSS treatment for serum and amino acid deprivation (−AA/GF) ($n = 6$). (F) Schematic representation of the role of SIRT4 in regulating the nutrient-dependent activation of mTORC1. The presence of SIRT4, even under low-glucose conditions, activates mTORC1, whereas knockdown under high-glucose conditions leads to attenuated mTORC1. The data represent means ± the SD (*, $P < 0.05$; **, $P < 0.005$; ***, $P < 0.001$; #, $P < 0.05$ compared to −AA/GF Ctrl).

tiating or eliciting maximal TORC1 signaling. Interestingly, ectopic expression of SIRT4 under low-glucose conditions, when its expression is otherwise diminished, significantly upregulated TORC1-mediated phosphorylation of S6K across various cell types, including in primary hepatocytes (Fig. 3A to C). Notably, this was comparable to signaling in control-transfected cells, which were grown under high-glucose conditions. Importantly, $SIRT4^{-/-}$ hepatocytes under both low- and high-glucose conditions exhibit a robust decrease in pS6K, which was rescued upon SIRT4 expression (Fig. 3D), and this was reminiscent of control-transfected cells grown in low-glucose medium (Fig. 3C). These results clearly indicated that whereas ectopic expression of SIRT4 mimics mTORC1 signaling under a high-nutrient state, its knockdown phenocopied signaling in low-glucose conditions.

Next, given that nutrients and growth factors in the serum are potent activators of mTOR, we wanted to assess the interplay between serum/amino acid inputs and SIRT4 in regulating TORC1 signaling. As expected, serum and amino acid deprivation led to a stark decrease in TORC1 signaling in both control and SIRT4-transfected cells (Fig. 3E). Despite this decrease, we noticed that pS6K levels were still higher, albeit marginally, in SIRT4-transfected cells after serum and amino acid withdrawal, compared to control transfected cells (Fig. 3E). This finding was interesting and indicated that ectopic expression of SIRT4 led to sustenance of TORC1 signaling even after upstream inputs were withdrawn. This could also have possibly arisen due to delayed attenuation kinetics of mTOR signaling, which needs to be investigated in the future. These results

clearly indicate that the levels of SIRT4 lead to differential TORC1 signaling in response to various inputs, which have been otherwise shown to be key for TORC1 activation. Importantly, SIRT4 seems to potentiate and thus regulate anabolic signaling mediated by TORC1.

SIRT4-dependent glutamine sparing mediates TORC1 activation. It was striking to note the similarity between the glutamine-mediated increase in TORC1 signaling under high-glucose conditions and a SIRT4-dependent response under low-glucose conditions (Fig. 1 and 2). This prompted us to ask whether SIRT4, whose expression is highest under a fed state, exerted control over TORC1 signaling via glutamine. Inhibiting mitochondrial glutamine utilization in control transfected cells, using EGCG or BPTES (inhibitors of GDH and GLS, respectively), as shown earlier (Fig. 1C and D), led to significant increase in pS6K levels, and this increase was comparable to that observed in cells transfected with SIRT4 (Fig. 4A and B). Interestingly, EGCG and BPTES treatments in SIRT4-transfected cells led to a further increase in TORC1 signaling, as assessed by pS6K/S6K ratios. This strongly suggested, for most part, the likelihood of SIRT4-dependent regulation of TORC1 being brought about by differential utilization of glutamine in the mitochondria. Moreover, earlier studies both in cancers and in beta islets have clearly established SIRT4 as a key factor in regulating glutamine utilization via the TCA cycle, which is brought about by SIRT4-mediated inhibition of GDH activity (22, 36). Thus, we hypothesized that mechanistically SIRT4-dependent glutamine sparing by the mitochondria might activate TORC1, as under a fed state.

Toward this, we first checked whether the observed effects of SIRT4 on TORC1 were because of altered glutamine channeling into the TCA cycle, specifically under low-glucose conditions. As expected, we found that glutamine supplementation led to elevated α-KG levels, which was accompanied by a small increase in TORC1 signaling in control cells (Fig. 4C). α-KG levels did not decrease upon SIRT4 overexpression in low-glucose medium without glutamine supplementation; nonetheless, this led to activation of TORC1 (Fig. 4C). However, it is important to note that unlike in control cells, while α-KG levels did not increase in SIRT4-transfected cells after glutamine supplementation, phosphorylation of S6K was significantly higher (Fig. 4C). Thus, the reciprocal changes in glutamine utilization and extent of S6K phosphorylation, which was dependent upon SIRT4 expression, clearly indicated that differential channeling of glutamine into TCA cycle-regulated TORC1 in the cytosol (Fig. 4C and D). Importantly, rescuing SIRT4 in primary hepatocytes isolated from $SIRT4^{-/-}$ mice, which results in rescue of pS6K to wild-type levels (Fig. 2J), led to a similar response to glutamine, as seen in hepatocytes derived from wild-type mice (Fig. 4E).

To gain further insights into the state of glutamine flux into the TCA in $SIRT4^{-/-}$ cells, we used a targeted liquid chromatography-tandem mass spectrometry (LC-MS/MS)-based metabolite analysis on wild-type and $SIRT4^{-/-}$ hepatocytes grown under high-glucose conditions. Although we did not observe a decrease in glutamine levels in $SIRT4^{-/-}$ cells (Fig. 4F), likely due to these cells being grown in glutamine-rich medium, we observed a robust increase in the steady-state amounts of α-KG (Fig. 4F), as well as glutamate (Fig. 4F), in $SIRT4^{-/-}$ hepatocytes compared to the wild type. Importantly, such an increase in the α-KG/glutamate ratio (Fig. 4G) and a decrease in the glutamine/glutamate ratio (Fig. 4H) is strongly consistent with our hypothesis of increased flux of glutamine to feed the TCA cycle in $SIRT4^{-/-}$ hepatocytes. We also observed a striking increase in TCA intermediates downstream of α-KG, in $SIRT4^{-/-}$ hepatocytes, suggesting very high TCA flux in the system (Fig. 4F), which is typically indicative of (i) higher mitochondrial GTP and (ii) the cells being in a constitutively high mitochondrial activity state. However, notably, despite this high flux (and possible high level of GTP, a potent inhibitor of GDH activity), the absence of SIRT4 consistently results in enhanced GDH activity (Fig. 4H) (22).

Although the results presented above clearly indicated SIRT4-dependent glutamine utilization in the mitochondria to be pivotal for TORC1 signaling, we wanted to provide conclusive mechanistic evidence. Specifically, we assessed if metabolic compensation
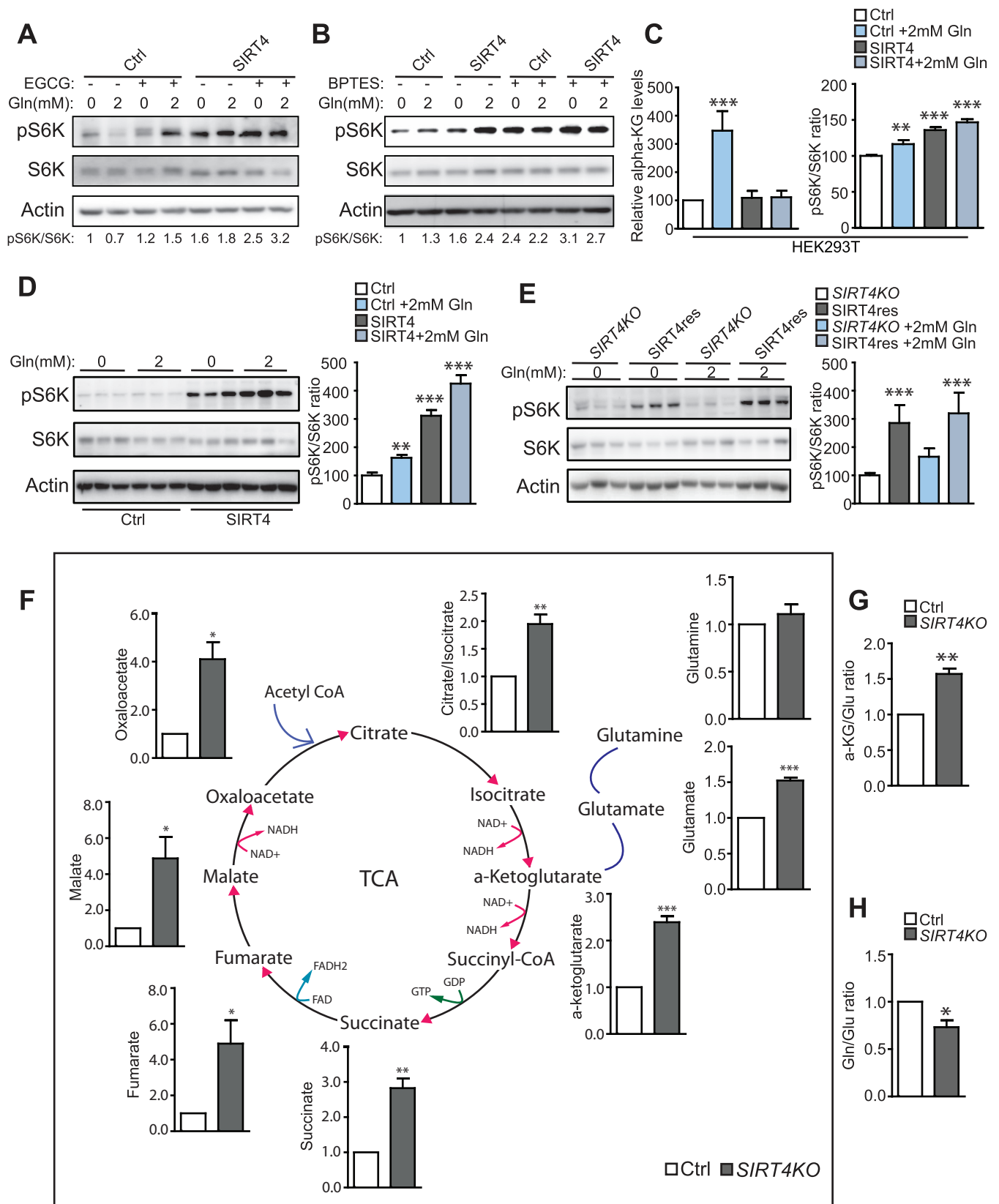
FIG 4 SIRT4-dependent glutamine sparing mediates TORC1 activation. (A and B) Representative immunoblots for pS6K/S6K and actin in primary hepatocytes derived from wild-type mice were adenovirally transduced with control or SIRT4 and incubated in low (5 mM)-glucose medium with or without 2 mM glutamine and 100 μM EGCG (A) or 20 μM BPTES (B), as indicated. (C) Relative α-ketoglutarate levels in control (Ctrl) and SIRT4-transfected (SIRT4) HEK293T cells ($n = 3$) and quantitations for pS6K/S6K in control (Ctrl) and SIRT4-transfected (SIRT4) HEK293T cells ($n = 4$) incubated in 5 mM glucose-containing medium with or
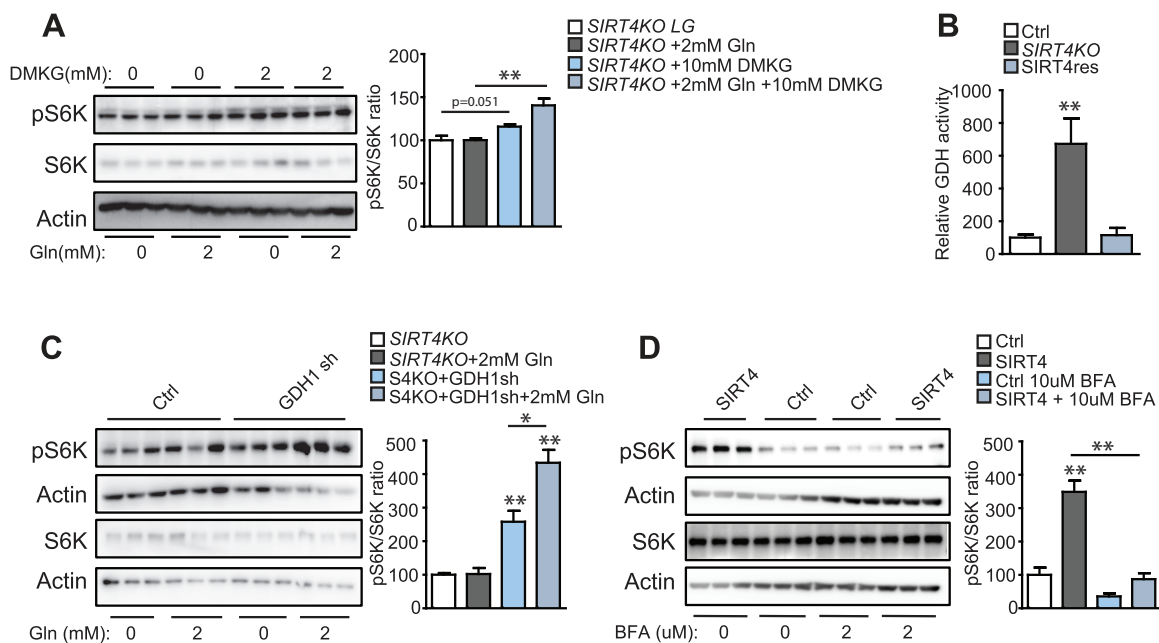
(Continued on next page)

FIG 5 SIRT4-mediated regulation of anaplerotic flux activates mTORC1. (A) Representative immunoblots of pS6K/S6K in SIRT4KO hepatocytes treated with 2 mM glutamine (Gln) and/or 10 mM dimethyl α-ketoglutarate (DMKG) ($n = 4$). (B) Relative glutamate dehydrogenase (GDH) activity in primary hepatocytes isolated from wild-type and SIRT4KO mice. SIRT4 expression was restored by transducing Ad-SIRT4 in SIRT4KO hepatocytes (SIRT4res) ($n = 3$). (C and D) Representative immunoblots for pS6K/S6K in SIRT-4KO hepatocytes transduced with Ad-CMV adenovirally and/or GDH1sh lentivirus and kept in low-glucose medium for 1 h with or without glutamine supplementation ($n = 6$) (C) and wild-type hepatocytes adenovirally transduced with Ad-CMV (Ctrl) or Ad-SIRT4 (SIRT4) treated with 10 μM brefeldin A in low-glucose conditions for 1 h ($n = 6$) (D). The data represent means ± the SD (*, $P < 0.005$; **, $P < 0.001$).

with dimethyl α-ketoglutarate (DMKG), a cell-permeable analog of α-ketoglutarate, would now lead to glutamine sparing and thus restore TORC1 signaling in $SIRT4^{-/-}$ hepatocytes. As hypothesized, glutamine supplementation activated mTORC1 significantly only when DMKG was simultaneously administered to these cells. This indicated that bypassing glutamine utilization by anaplerotic flux by DMKG was sufficient to spare glutamine for mTORC1 activation. (Fig. 5A). These findings were corroborated by enhanced GDH activity in primary hepatocytes from $SIRT4^{-/-}$ mice, which was reduced to control levels when SIRT4 expression was restored (Fig. 5B). Hence, as also indicated by the experiments with EGCG, knockdown of GDH1 in $SIRT4^{-/-}$ hepatocytes led to a robust increase in pS6K levels which were further enhanced by glutamine addition under low-glucose conditions, in contrast to just $SIRT4^{-/-}$ hepatocytes (Fig. 5C).

Glutamine-dependent TORC1 activation has been established to be mediated via Arf1 GTPase, which enhances lysosomal localization of mTOR (17). Thus, to confirm the importance of the SIRT4/GDH/glutamine axis in regulating TORC1, we inhibited Arf1 GTPase by brefeldin A in control and SIRT4-overexpressing hepatocytes under low-glucose conditions. Notably, Arf1 inhibition abrogated the SIRT4-mediated increase in TORC1 signaling (Fig. 5D). Together, our biochemical, genetic, and pharmacological approaches clearly demonstrate that SIRT4-mediated "glutamine sparing" contributes to TORC1 activation.

The SIRT4-AMPK axis also exerts control over TORC1 signaling. We have earlier established that an interplay between SIRT4-ANT2 is necessary to maintain cellular energetics (20). Specifically, the absence of SIRT4 results in reduced cellular ATP (and an

FIG 4 Legend (Continued)

without 2 mM glutamine supplementation. (D and E) Immunoblots and quantitations for pS6K/S6K and actin in primary hepatocytes derived from wild-type ($n = 5$) (D) and SIRT4KO mice ($n = 6$) (E) and adenovirally transduced with Ad-CMV (Ctrl) or Ad-SIRT4 (SIRT4/SIRT4res). All experiments with glutamine were performed at 2 mM glutamine (2 mM Gln) given in 5 mM glucose medium for 1 h. (F) Relative levels of TCA cycle metabolites, glutamate, and glutamine in wild-type and SIRT4KO hepatocytes ($n = 5$). (G and H) α-Ketoglutarate/glutamate (G) and glutamine/glutamate (H) ratios in wild-type and SIRT4KO hepatocytes ($n = 5$). The data represent means ± the SD (*, $P < 0.05$; **, $P < 0.005$; ***, $P < 0.001$).

increase in the AMP/ATP ratio) and thus the activation of AMPK, which is an upstream inhibitor of TORC1 (37). Recent reports have also indicated that ATP is a potent activator of mTOR (38). Moreover, the additive increase in pS6K after glutamine and SIRT4 supplementation (Fig. 4 and 5) posited a role for a SIRT4-mediated dual control in eliciting TORC1 activation. We surmised that physiologically it is logical to expect both metabolic (amino acid mediated) and energetic cues as being critical modulators of anabolic signaling via mTOR.

Thus, we wanted to assess whether SIRT4-mediated inhibition of AMPK also contributed to TORC1 activation. Activation of AMPK by AICAR led to a drastic reduction in pS6K in both control and SIRT4-overexpressing cells (Fig. 6A), and this decrease was not rescued by glutamine supplementation. This was not surprising since AMPK is known to inhibit mTORC1 upstream to glutamine (39). In order to assess whether subliminal activation of AMPK could be rescued by glutamine sparing, we activated AMPK by a lower dose of AICAR in $SIRT4^{-/-}$ and SIRT4-rescued hepatocytes (Fig. 6D). Slight AMPK activation in $SIRT4^{-/-}$ cells did not lead to a significant change in pS6K levels compared to control hepatocytes, while in SIRT4-rescued cells it led to a reduction in pS6K compared to controls (Fig. 6C). Importantly, the addition of glutamine in low-dose AICAR-treated SIRT4-rescued cells restored TORC1 signaling. Conversely, inhibiting AMPK in $SIRT4^{-/-}$ hepatocytes using compound C led to an increase in pS6K levels. Notably, this was further enhanced upon SIRT4 rescue (Fig. 6E). Together, these results clearly established that SIRT4 exerted a dual control over TORC1 signaling, i.e., via both glutamine and AMPK. Our findings also point out possible thresholding effects of glutamine- and ATP-dependent regulation of TORC1, which could potentially result in a graded activation of anabolic pathways and would be addressed in the future. Such a hypothesis is supported by recent indications that TOR may be activated by coincidence detection of upstream cues (40, 41).

SIRT4 regulates mTOR localization to the lysosomes. Lysosomal localization of mTOR is essential for its activation (42), and since it is a direct readout of the extent of activation, we assessed the same as a function of SIRT4 expression in primary hepatocytes from control and $SIRT4^{-/-}$ mice. We observed a drastic reduction in mTOR puncta in $SIRT4^{-/-}$ hepatocytes compared to the wild type under low-glucose conditions, which was rescued upon SIRT4 expression (Fig. 7A and C). Importantly, there was a marked increase in mTOR intensity in glutamine supplemented SIRT4 overexpressing cells (Fig. 7B and C). These not only corroborated the biochemical data but also confirmed that SIRT4 was essential for activation of anabolic signaling via TORC1. We also assessed mTOR levels in wild-type and $SIRT4^{-/-}$ hepatocytes and did not find a significant reduction in the levels of mTOR protein, indicating that attenuated mTORC1 activation in $SIRT4^{-/-}$ hepatocytes is due to decreased signaling (Fig. 7D).

The SIRT4-TOR axis impinges on transcription via SREBP1 activation. In lipogenic cells, activation of SREBP1c, the master transcriptional regulator of lipid metabolism, is primarily dependent on TORC1 activity (43). Although others and we have previously established SIRT4 as a negative regulator of transcription of fatty acid oxidation genes, if or how it controls transcription of lipogenic genes is still unknown. Thus, we assessed whether the SIRT4-TORC1 axis leads to SREBP1c activation, again specifically under low-glucose conditions to negate for other inputs. Ectopic expression of SIRT4 led to a robust increase in luciferase expression downstream of FAS (fatty acid synthetase) promoter under low-glucose conditions, which was equivalent to high-glucose states (Fig. 8A). Further, we found that the endogenous levels of transcripts of lipogenic genes, such as those for FAS and SCD1 (stearyl coenzyme A desaturase), were low in $SIRT4^{-/-}$ hepatocytes (Fig. 8B). Importantly, the expression of these SREBP1c target genes was restored to wild-type levels when SIRT4 expression was rescued in $SIRT4^{-/-}$ hepatocytes (Fig. 8B). Interestingly, glutamine supplementation to cells overexpressing SIRT4 led to a robust increase in FAS expression even under low-glucose conditions (Fig. 8C). However, glutamine supplementation to $SIRT4^{-/-}$ hepatocytes led to no increase in FAS expression, which was rescued upon SIRT4 restoration (Fig. 8D). Further, on assaying for lipid content by oil red staining, we found that
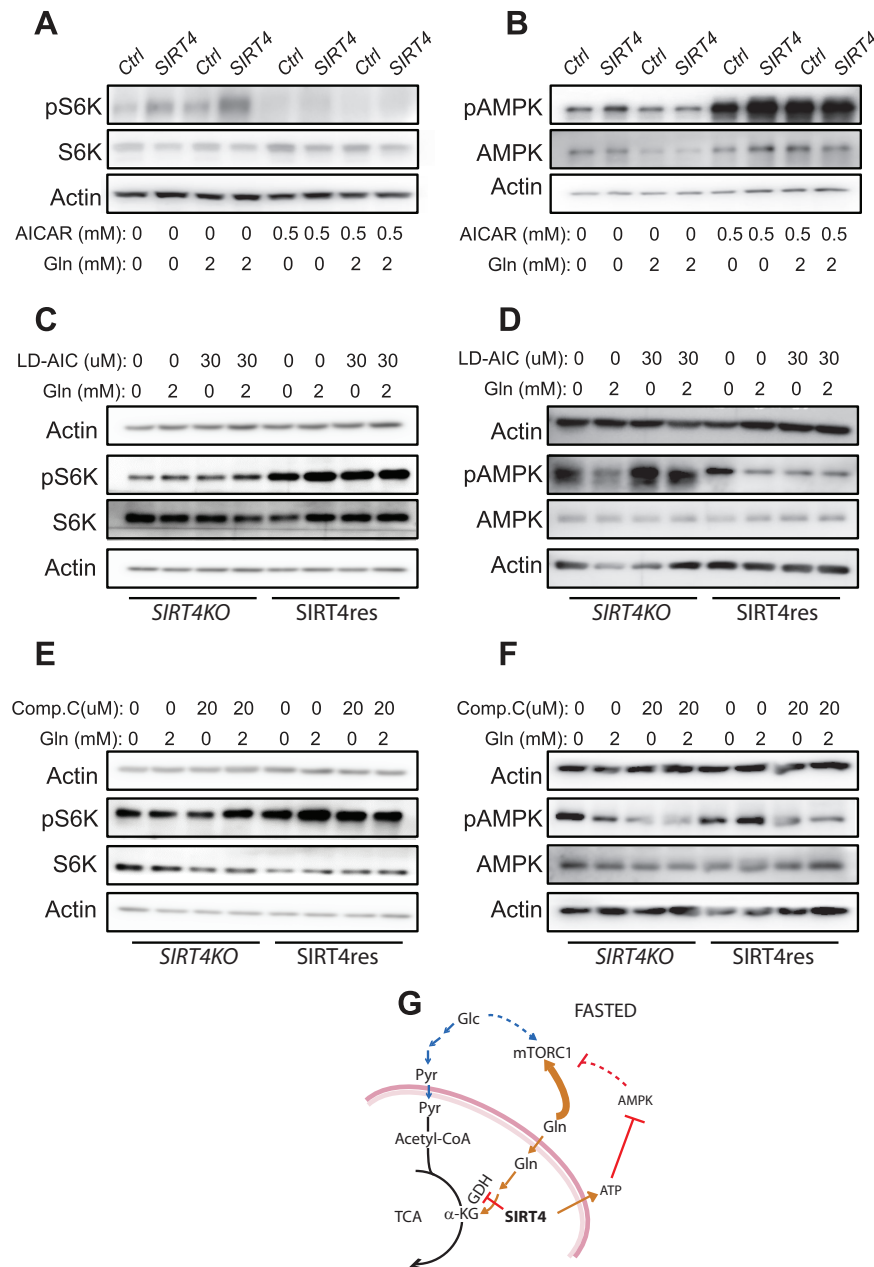
FIG 6 The SIRT4-AMPK axis also exerts control over TORC1 signaling. (A and B) Representative immunoblots for pS6K/S6K (A) and pAMPK/AMPK (B) in primary hepatocytes transduced with Ad-CMV (Ctrl) or Ad-SIRT4 (SIRT4) and incubated in 5 mM glucose medium with or without 2 mM glutamine and/or 0.5 mM AICAR for 1 h ($n = 4$). (C and D) Representative immunoblots for pS6K/S6K (C) and pAMPK/AMPK (D) in SIRT4KO hepatocytes transduced with Ad-CMV (Ctrl) or Ad-SIRT4 (SIRT4res) and incubated in 5 mM glucose medium with or without 2 mM glutamine and/or 0.03 mM AICAR for 1 h ($n = 4$). (E and F) Representative immunoblots for pS6K/S6K (E) and pAMPK/AMPK (F) in SIRT4KO hepatocytes transduced with Ad-CMV (Ctrl) or Ad-SIRT4 (SIRT4res) and incubated in 5 mM glucose medium with or without 2 mM glutamine and/or 20 μM compound C for 1 h ($n = 4$). (G) Schematic representation of a change in anaplerotic flux driven by SIRT4, leading to mTORC1 activation even under a fasted state. SIRT4 expression leads to increased ATP levels in the cell, which lead in turn to reduced AMPK activation and further derepression of mTORC1 activity.

$SIRT4^{-/-}$ hepatocytes had a reduced level of lipid droplets, which was again restored to control level after the rescue of SIRT4 expression (Fig. 8E). These findings clearly demonstrate that SIRT4 activates the lipogenic response in hepatocytes and, together with previous findings (32), indicate that SIRT4 maintains the balance between lipid synthesis and breakdown.
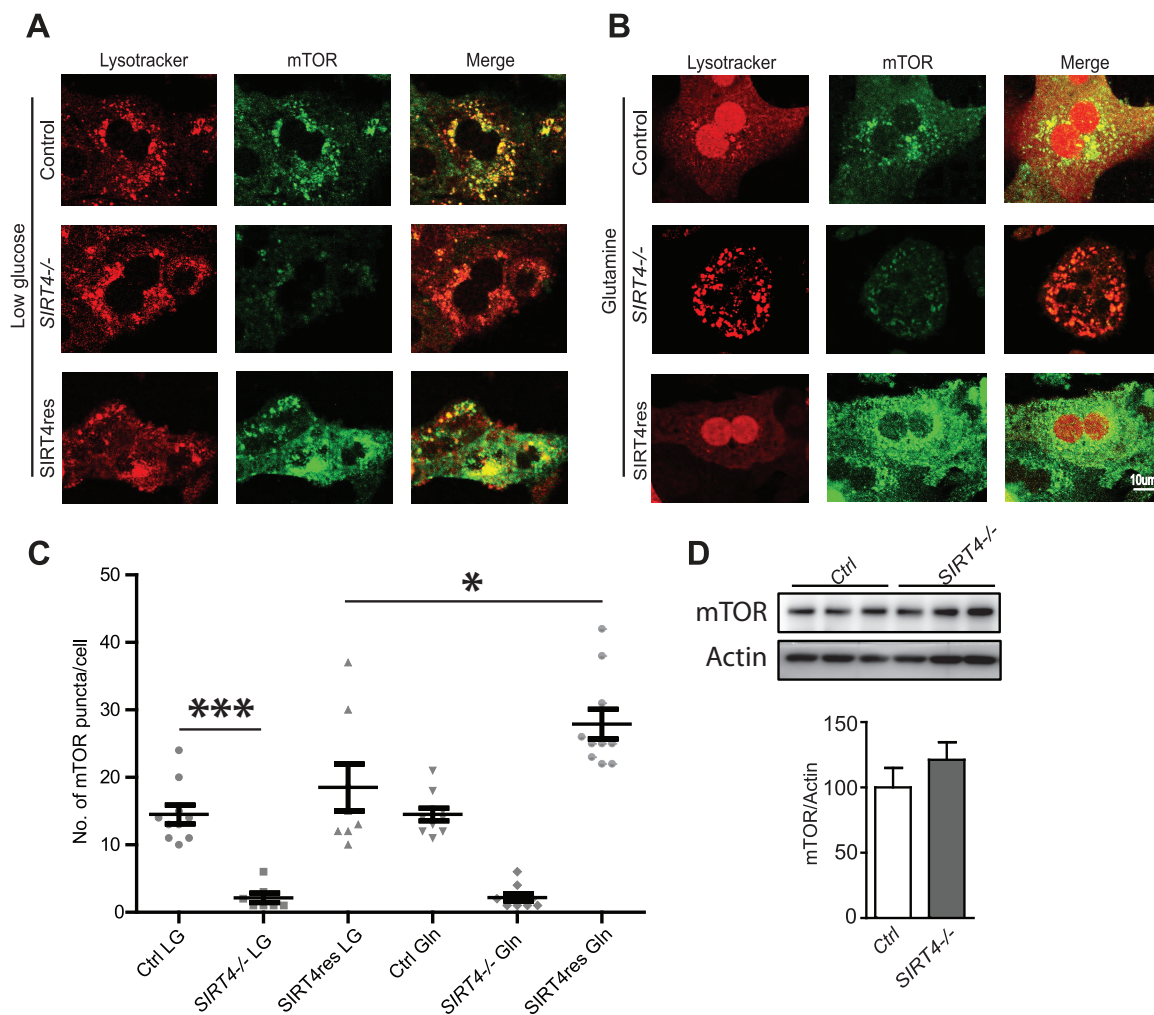
FIG 7 Sirt4 regulates mTORC1 localization to the lysosomes. (A to C) Immunofluorescence images and quantitation of mTOR puncta (green) in primary hepatocytes derived from wild-type and $SIRT4^{-/-}$ (SIRT4KO) mice adenovirally transduced with Ad-CMV (Ctrl) or Ad-SIRT4 (SIRT4res) and treated with 2 mM glutamine under low-glucose (5 mM) conditions for 1 h. (D) Representative immunoblots for mTOR and actin in wild-type and SIRT4KO hepatocytes ($n = 4$). The data represent means ± the standard errors of the mean (SEM; *, $P < 0.05$; ***, $P < 0.001$).

Anabolic SIRT4 exerts control over autophagy and cell proliferation. Balance between AMPK and mTOR (specifically TORC1) signaling is critical to couple cellular metabolic/energetic state to catabolic/anabolic pathways, which determine processes such as autophagy and cell proliferation/growth. Taking together our previous report on SIRT4-dependent inhibition of AMPK and the current findings on the ability of SIRT4 to activate TORC1, we wanted to assess the physiological relevance of SIRT4 expression. Specifically, we wanted to ascertain whether anabolic SIRT4 could impinge on autophagy and cell proliferation.

On assessing the ratio of LC3-II to actin, an indicator of autophagy, we saw a significant decrease in LC-II/actin in SIRT4-overexpressing cells (Fig. 9A). Conversely, there was a robust increase in LC3-II/actin ratio in SIRT4 knockdown cells (Fig. 9B). Although the LC3-II levels are indicative of the extent of autophagy, they are not confirmatory. As established, we checked the autophagy flux by treating cells with leupeptin, which inhibits lysosomal proteases (44), and assaying for the LC3-II/actin ratio. Consistent with the literature, we observed a high autophagy flux in control transfected cells under low-glucose conditions (Fig. 9C). Interestingly, ectopic expression of SIRT4 under low-glucose conditions dampened this response (Fig. 9D) and was comparable to autophagy flux of control transfected cells grown in medium
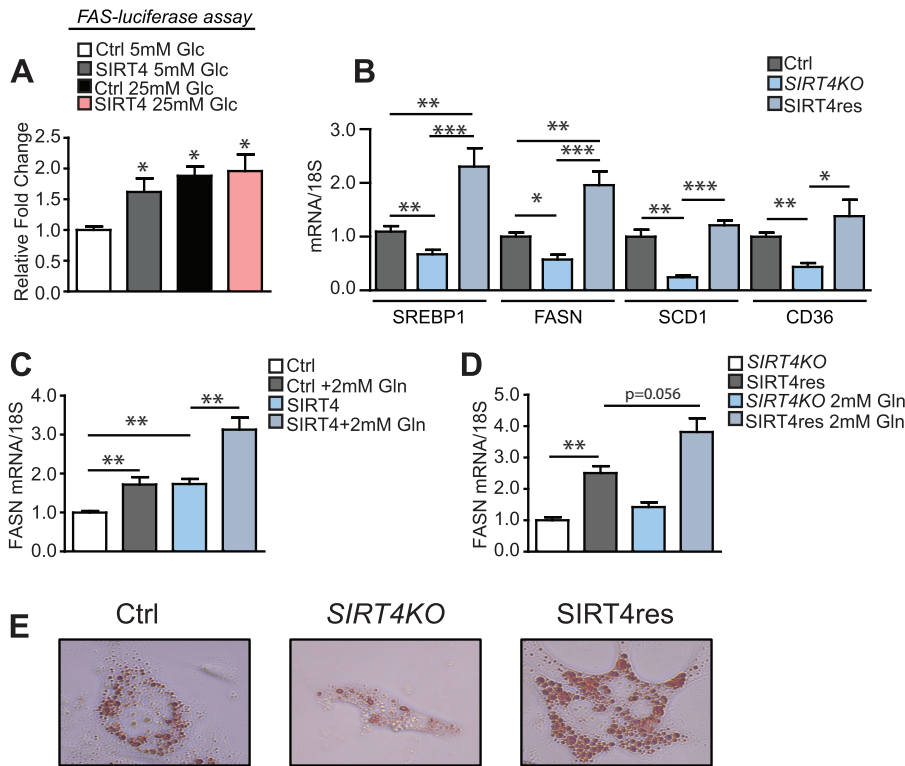
FIG 8 The Sirt4-TOR axis impinges on transcription via SREBP1 activation. (A) FAS promoter-driven luciferase assay in HepG2 cells overexpressing SIRT4 in 5 and 25 mM glucose medium conditions ($n = 6$). (B) Quantitative RT-PCR of genes involved in lipogenesis and fatty acid uptake (SREBP1, FASN, SCD1, and CD36) from primary hepatocytes isolated from wild-type (Ctrl), $SIRT4^{-/-}$ (SIRT4KO), and Ad-SIRT4 transduced SIRT4KO (SIRT4res) ($n = 4$ to 6). (C and D) Quantitative RT-PCR of FASN in primary hepatocytes derived from wild-type (C) and $SIRT4^{-/-}$ (D) mice adenovirally transduced with either Ad-CMV (Ctrl/$SIRT4KO$) or Ad-SIRT4 (SIRT4/SIRT4res) and treated with 2 mM glutamine in low (5 mM)-glucose medium for 6 h ($n = 5$ or 6). (E) Representative images for Oil Red O staining of primary hepatocytes derived from wild-type (Ctrl), $SIRT4^{-/-}$ (SIRT4KO), and Ad-SIRT4-transduced $SIRT4^{-/-}$ hepatocytes (SIRT4res) kept for 12 h under low-glucose (5 mM) conditions. Magnification, ×40. Statistical significance was calculated by using a Student t test and ANOVA (*, $P < 0.05$; **, $P < 0.01$; ***, $P < 0.001$). Error bars indicate means ± the SEM.

containing high levels of glucose (Fig. 9E). On the other hand, knocking down SIRT4 expression in cells grown in high-glucose medium led to a significant increase in LC3-II (Fig. 9F), which was similar to control transfected cells under low-glucose conditions (Fig. 9C). In addition, imaging LC3 puncta in wild-type and $SIRT4^{-/-}$ hepatocytes indicated an increased autophagic flux in $SIRT4^{-/-}$ hepatocytes (Fig. 9G). These findings clearly indicated that the presence or absence of SIRT4 affected cellular autophagy and mimicked either a fed or fasted state, respectively, and were consistent with a change in TORC1 signaling (Fig. 2).

In the context of autophagy, AMPK and TORC1 counteract each other by phosphorylating the common downstream substrate ULK1. Notably, TORC1-mediated inhibitory phosphorylation of ULK1 at Ser-757 (pULK757) has been shown to prevent AMPK-dependent activatory phosphorylation at Ser-317/777 (45). Thus, the effects of SIRT4 on autophagy are consistent with changes in the levels of pULK757 (Fig. 2E and H).

To get another correlate of SIRT4-dependent effects on cellular physiology, we scored for cell proliferation, which is again inherently linked with AMPK and mTOR activities (46). As anticipated, although cells expressing SIRT4 were more proliferative (Fig. 9H), knocking down SIRT4 led to reduced proliferation compared to the respective controls (Fig. 9I). This was again consistent with the ability of SIRT4 to induce anabolic signaling with TORC1.
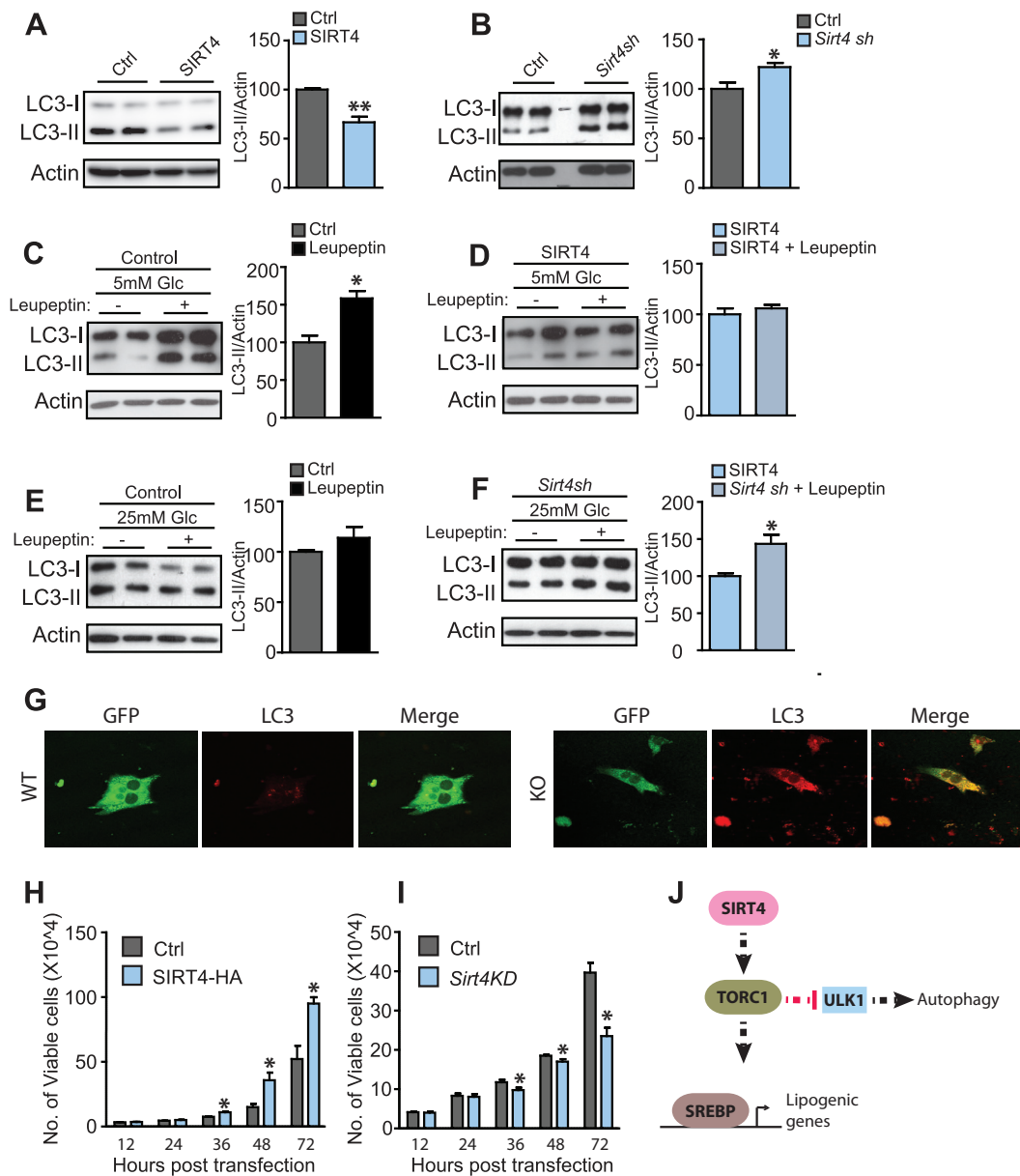
FIG 9 Anabolic SIRT4 exerts control over autophagy and cell proliferation. (A and B) Representative immunoblots and quantitations for LC3-II/actin in HEK293T cells transfected with control and SIRT4 overexpression vectors and kept in low (5 mM)-glucose medium (A) or control and SIRT4 knockdown vectors and and kept in high (25 mM)-glucose medium (B). (C and D) Representative immunoblots and quantitations for LC3-II/actin in control transfected (C) or SIRT4-overexpressing (D) HEK293T cells maintained in low (5 mM)-glucose medium with or without 100 μM leupeptin treatment for 12 h. (E and F) Representative immunoblots and quantitations for LC3-II/actin in control knockdown (E) or SIRT4-knockdown (F) HEK293T cells maintained in high (25 mM)-glucose medium with or without 100 μM leupeptin treatment for 12 h. (G) Representative immunofluorescence images of LC3 staining in Ad-CMV-transduced wild-type and SIRT4KO hepatocytes and kept in low-glucose medium. (H and I) Proliferation assay showing the number of cells in HEK293T cells transiently transfected with control and SIRT4-HA (H) and in control and Sirt4 knockdown (Sirt4KD) HEK293T cells (I) at different time points after plating. (J) Schematic representation of SIRT4-mediated control of lipogenesis and autophagy via the mTORC1-SREBP1 and mTORC1-ULK1 axes, respectively. The statistical significance was calculated using the Student t test and ANOVA (*, $P < 0.05$; **, $P < 0.01$). Error bars indicate means ± the SEM.

DISCUSSION

Catabolic and anabolic pathways/processes are intrinsically dependent upon the ability of cells to sense nutrient availability and have been largely studied under deprivation conditions. However, if and how intracellular utilization of one macronutrient affects the ability of the other to impinge on metabolic signaling are relatively less understood. Specifically, glutamine is utilized via anaplerotic pathways under

starvation (47) and is also known to activate mTOR signaling (17, 18). Hence, whether differential glutamine utilization in the mitochondria, which is dependent upon fed or fasted state of the cell, affects cytosolic TOR is still unclear. Here, we have demonstrated that glutamine sparing by the mitochondria is key for TORC1 activation. Importantly, we establish that SIRT4, a sirtuin that is particularly abundant in the fed state, plays a crucial role in regulating TORC1 signaling through glutamine utilization in the mitochondria.

Despite several studies, SIRT4 activity and its functions have remained enigmatic. More importantly, unlike all other sirtuins, which are induced in a fasted state, SIRT4 expression is highest in a fed state (20). As emphasized earlier, SIRT4 has only been described for its role as an anticatabolic factor (25, 32). Given this, we report its role as a mediator of anabolic signaling via TORC1, which was hitherto unknown. In this context, we have assessed the importance of SIRT4-dependent activation of anabolic TORC1 in lipogenesis, cell proliferation, and autophagy. We conclusively show that while SIRT4 enhances lipogenesis and cell proliferation, it downregulates autophagy. Others and we have established that the anticatabolic role of SIRT4 is mediated via the inhibition of AMPK, PGC1α, SIRT1, and peroxisome proliferator-activated receptor α (PPARα) (20, 25), factors that are also known to affect lipogenesis, cell proliferation, and autophagy (48–50). Together with our earlier study, which established SIRT4 as a negative regulator of AMPK signaling (20), we now propose SIRT4 activity in the mitochondria as a key determinant of the balance between cellular catabolic and anabolic pathways exerted via AMPK and TORC1. This is particularly evident by SIRT4-dependent change in the phosphorylation status of ULK1, a substrate of both AMPK and TORC1, in favor of TORC1-mediated modification at Ser-757. It should be noted that phosphorylation at Ser-757 is known to abrogate AMPK dependent phosphorylation of ULK1, which is activatory (45). In addition to highlighting the role of SIRT4 in AMPK-TORC1 balance, it also provides mechanistic basis to the ability of SIRT4 to regulate autophagy.

Loss of SIRT4 has been established to reduce body fat and protect from high-fat-induced obesity (32). Although others and we have shown that inhibiting fatty acid oxidation through the AMPK/PGC1α-SIRT1/PPARα axis is responsible for this phenotype (20, 25), if and how SIRT4 affects lipogenesis have not been addressed thus far. In this context, we found that SIRT4-TORC1 interplay regulates expression of lipogenic genes downstream to SREBP1 in primary hepatocytes, and these are consistent with the lean phenotype observed in $SIRT4^{-/-}$ mice (32). Motivated by our findings, it will be exciting to perturb SIRT4 expression in lipogenic tissues and study its impact on organismal physiology in the future.

One of the key highlights of our study is the unraveling of mTOR regulation by mitochondrial glutamine sparing. Although glutamine deprivation studies indicated that it is a crucial upstream factor that is necessary to activate mTOR (17, 18), our findings clearly show that differential glutamine utilization, via the TCA, during fed and fasted states control TORC1 signaling. Although recent reports have indicated that α-KG could impinge on mTOR and organismal life span (19), α-KG has been shown to have both inhibitory and activatory effects on mTOR (18, 19). In this regard, we provide a physiologically relevant context to control of TORC1 by glutamine metabolism in the mitochondria. Notably, our results suggest that glutamine could be utilized as a metabolic signal to conditionally activate mTOR-dependent anabolic pathways, which is dictated by the presence or absence of other nutrients that sustain cellular energetic needs.

Even though differential glutamine channeling into TCA affecting mTOR is rather intuitive, it becomes essential to identify a molecular factor that couples cellular energetics and glutamine metabolism. In this context, we have discovered that mitochondrial sirtuin SIRT4, whose role as a regulator of glutamine metabolism has been thoroughly established particularly in cancers (28), plays a pivotal role. We clearly demonstrate that the presence or absence of SIRT4 affects glutamine metabolism via glutamate dehydrogenase and thus the differential channeling of glutamine into the

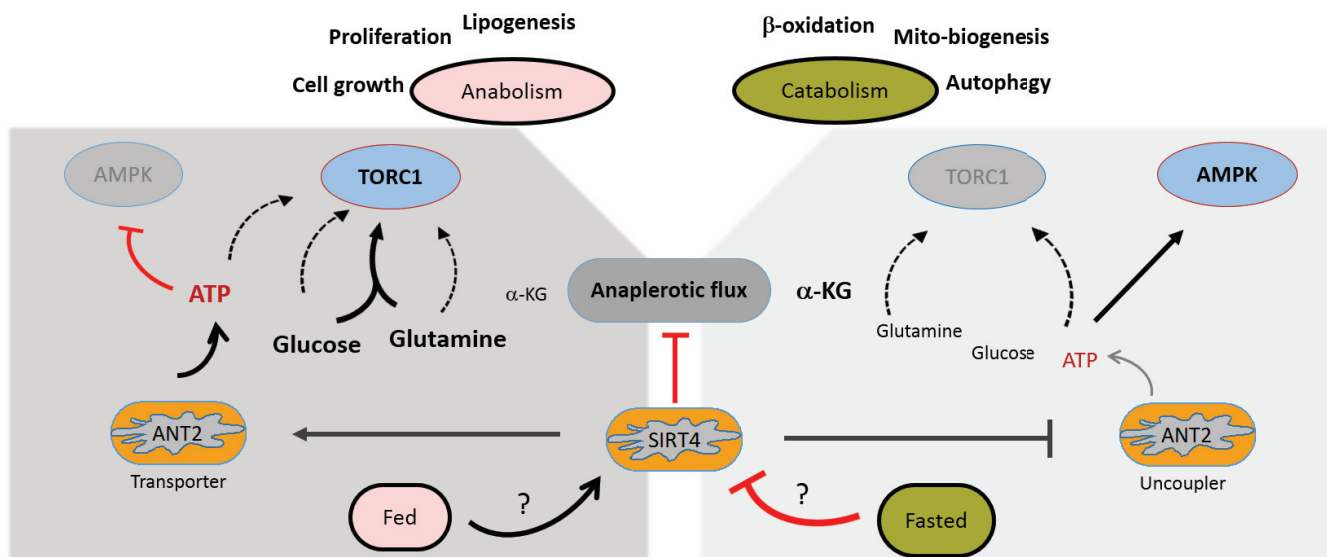## Anabolic SIRT4 activates TORCI via mitochondrial glutamine sparing

FIG 10 Schematic representation of mitochondrial regulation of nutrient dependent TORC1 signaling by SIRT4. SIRT4 modulates mitochondrial utilization of glutamine, which impinges on mTORC1 activation under a fasted-to-fed transition. Under fed states, inhibition of anaplerotic flux (via inhibition of GDH) by SIRT4 leads to spared glutamine in the cytosol, which then activates mTORC1. Under fasted states, when SIRT4 is low, increased GDH activation leads to the conversion of glutamine to α-KG and thus the inhibition of mTORC1 activity.

TCA through α-KG determines whether or not TORC1 should be induced (Fig. 10). It is worth noting that (i) our metabolite profiling in wild-type and SIRT4 knockout (SIRT4KO) hepatocytes clearly indicated reduced channeling of glutamine into TCA in the presence of SIRT4, (ii) we observed that a rescue of anaplerotic flux using methyl-α-KG (in SIRT4KO cells) resulted in the restoration of TORC1 signaling, and (iii) chemical or genetic perturbation of GDH highlighted that its interplay with SIRT4 was critical in eliciting control over TORC1. Further, based on the metabolite analyses, we also ruled out the possibility of GDH regulation via GTP in the absence of SIRT4. Thus, we provide conclusive mechanistic support to explain both glutamine sparing-mediated and SIRT4-dependent activation of TORC1.

Moreover, based on our earlier study wherein we had identified SIRT4 to be a negative regulator of AMPK and the results described here, we show that SIRT4 exerts control over TORC1 via both AMPK and glutamine. This is interesting since glutamine utilization is intrinsically coupled to cellular energetics, as mentioned earlier (31). Therefore, it is likely that glutamine sparing and mitochondrial ATP production, which affects AMPK signaling, might synergistically bring about multiple dynamic states of mTOR/TORC1 activation. As mentioned earlier, this is exciting since mitochondrial control of anabolic pathways, via TORC1, could be tuned variably based on metabolite availability (i.e., glutamine) and energetic status (via ATP/AMPK).

Emerging literature indicates that both extent of TORC1 activation and differential phosphorylation of downstream substrates are crucial for encoding specificity (33, 35, 51). In this regard, it is interesting to note that SIRT4-mediated control of mTOR is limited to TORC1-dependent phosphorylation of S6K and ULK1 but not 4E-BP1. It should be noted that Kang et al. reported that 4E-BP1, a high-affinity substrate, is also resistant to TORC1 inhibition (33, 34), analogous to our findings. Hence, it will be exciting to address, in the future, the differential control of mTOR-dependent processes by mitochondrial signals and the impact on cellular growth and proliferation.

Our study also distinguishes the cross talk between metabolic inputs, SIRT4 functions, and cellular physiology. Consistent with the regulation of TORC1 signaling via

glutamine sparing, we have found that it is indeed differential SIRT4 expression under low- or high-glucose conditions, which determines the ability of cells to mount TORC1 signaling. Specifically, it should be noted that absence of SIRT4 led to a drastic reduction in TORC1 signaling even under high-glucose conditions and ectopic expression of SIRT4 under low-glucose conditions mimicked GDH inhibited state vis-à-vis effects on TORC1. These are also supported by changes in autophagy as a function of SIRT4 expression under both high- and low-glucose conditions.

In conclusion, by identifying SIRT4 as a key determinant of TORC1 signaling, we have provided molecular and physiological basis for mitochondrial control of mTOR. Being the first report to describe the dependence of anabolic signaling on SIRT4, we believe that this will motivate further studies in unraveling the need for a sirtuin to be induced during a nutrient-rich state.

MATERIALS AND METHODS

Cell lines and primary hepatocyte culture. HEK293, HEK293T and HepG2 cell lines were obtained from ATCC and were maintained in Dulbecco modified Eagle medium (DMEM; Sigma, catalog no. D7777) containing 25 mM glucose with 10% fetal bovine serum (FBS; Gibco, catalog no. 16000-044) unless otherwise stated. The HHL-17 cell line was kindly provided by Arvind Patel (MRC-University of Glasgow Centre for Virus Research).

Primary hepatocyte isolation. Primary hepatocytes were isolated from 3- to 4-month-old, male, wild-type and *SIRT4* knockout (*SIRT4*$^{-/-}$) mice (obtained from Jackson Laboratories, catalog no. 012756), maintained under standard animal house conditions and fed with standard chow diet. Animals were sedated using thiopentone and perfused through the portal vein with Hanks balanced salt solution, followed by low-glucose DMEM containing collagenase A (340 μg/ml; Sigma-Aldrich, catalog no. C5138). The tissue was minced in this solution and passed through a 70-μm-pore size strainer to obtain a single cell suspension. This suspension was then centrifuged at 50 $\times$ *g* and 4°C for 5 min. The pellet was washed twice and plated at desired density in high-glucose DMEM with 10% FBS in collagen type I (Sigma-Aldrich, catalog no. C3867)-coated plates. The medium was changed to serum-free medium after 6 h of plating. All animal studies were performed using Institutional Animal Ethics Committee (IAEC)-approved protocols.

Plasmids and constructs. Human SIRT4 cDNA was cloned into pBabe-puro. pLKO.1-eGFP scrambled shRNA was a gift from Sorab Dalal (ACTREC, India). pLKO.1 Sirt4 shRNA (TRC0000018948) was purchased from Sigma-Aldrich. SIRT4 was cloned into pAdtrack CMV plasmid, which was a gift from Bert Vogelstein (Addgene, plasmid 16405).

Adenoviral and lentiviral preparation. SIRT4 was cloned into pAdtrack CMV plasmid, and adenovirus was prepared according to the protocol described by Luo et al. (52). Cells were collected after the expression of green fluorescent protein (GFP) and lysed using hypotonic buffer (100 mM HEPES [pH 7.5], 1.5 mM MgCl$_2$, 10 mM KCl, 0.5 mM dithiothreitol). The supernatant was collected and used for transduction in different cell types. SIRT4 expression was confirmed by reverse transcription-PCR (RT-PCR) or quantitative reverse transcription-PCR.

For lentiviral preparation, pLKO.1 scrambled shRNA or *Sirt4* shRNA was transfected in HEK293T cells with packaging plasmids pMD2.G (Addgene, plasmid 12259) and psPAX2 (Addgene, plasmid 12260), which were a gift from Didier Trono. Media were collected at 36 and 48 h posttransfection, filtered using 0.45-μm-pore-size filters, and stored at -80°C until use.

Transfection and transductions. Cells were transfected with plasmids as indicated using Lipofectamine 2000 (Invitrogen, catalog no. 11668019) according to the manufacturer's instructions. Adenoviral particles were used for transducing cell lines after 12 h of plating; the cells were collected 36 h postransduction after respective treatments. Primary hepatocyte cultures were transduced with adenovirus after 24 h of plating and collected 72 h postplating after respective treatments. Lentiviral particles were used for knockdown in cells after 24 h of plating in the presence of Polybrene (Sigma-Aldrich, catalog no. H9268) at a concentration of 8 μg/ml. Cells were collected at 48 h postransduction.

Treatments. All treatments were given in FBS-containing medium unless otherwise specified. For GDH inhibition experiments, epigallocatechin gallate (EGCG; Sigma-Aldrich, catalog no. E4143) was used at a concentration of 100 μM for 1 h in low (5 mM)-glucose medium. For GLS inhibition experiments, bis-2-(5-phenylacetamido-1,3,4-thiadiazol-2-yl)ethyl sulfide (BPTES; Sigma-Aldrich, catalog no. SML0601) was used at a concentration of 20 μM for 1 h in low (5 mM)-glucose medium. For experiments in low or high glucose, the cells were either shifted to 5 mM glucose-containing medium (low; Sigma, catalog no. D5523) or fresh 25 mM glucose-containing medium (high) 12 h prior to collection. For TOR inhibition, cells were treated with 20 nM rapamycin (Sigma, catalog no. 0395) for 30 min under low-glucose conditions. For amino acid and growth factor starvation, the cells were kept in 5 mM glucose containing DMEM for 3 h, followed by 1 h in serum-free Earle's balanced salt solution (EBSS; Sigma, catalog no. E2888) prior to collection. For glutamine supplementation experiments, cells were kept in 2 mM glutamine supplemented in 5 mM glucose- or 25 mM glucose-containing DMEM (as indicated in the figures) for 1 h. For the GDH assay, the cells were cultured in 5 mM glucose-containing DMEM. For AMPK activation, 0.5 mM AICAR (Sigma, catalog no. A9978) was used as a high dose, and 0.03 mM was used as a low dose for 1 h. For AMPK inhibition, compound C (dorsomorphin; Sigma, catalog no. A5499) was used at a 20 μM dose for 1 h. For increasing anaplerotic flux, 10 mM dimethyl α-ketoglutarate (DMKG; Sigma, catalog no. 349631) was added to cells for 1 h. For Arf1 inhibition, 10 μM

brefeldin A was added in low-glucose conditions for 1 h. For inhibition of autophagy flux, the cells were kept in either low (5 mM)- or high (25 mM)-glucose medium with or without 100 μM leupeptin (Sigma, catalog no. L2884) for 12 h. For the qPCR and luciferase assays, the cells were kept in the indicated medium conditions for 6 h.

Western blotting. Cells were lysed with radioimmunoprecipitation assay lysis buffer (50 mM Tris [pH 8], 150 mM sodium chloride, 0.1% SDS, 0.5% sodium deoxycholate, 1% Triton X-100, 1 mM sucrose) supplemented with protease inhibitor cocktail (Roche, catalog no. 04693159001), phosphatase inhibitor PhosSTOP (Roche, catalog no. 000000010837091001), and 1 mM phenylmethylsulfonyl fluoride (Sigma). The lysates were centrifuged at 12,000 rpm (4°C) for 10 min to remove cell debris. The concentration of protein was measured using the BCA protein assay kit (Thermo Fisher Scientific, catalog no. 23225). Subsequently, equal amounts of protein (in 1$\times$ Laemmli loading buffer) were resolved using SDS-PAGE gels and transferred to polyvinylidene difluoride membranes (Millipore, catalog no. IPVH00010). After blocking in 5% bovine serum albumin (BSA) or 5% fat-free milk in TBST (Tris-buffered saline with 0.1% Tween 20) for 1 h at room temperature, the membranes were incubated with primary antibody at 4°C overnight. To visualize the bands, the blots were incubated with horseradish peroxidase-conjugated secondary antibodies in 5% fat-free milk in TBST for 1 h at room temperature, followed by washes in TBST. Next, the membranes were visualized using the GE AI600 chemiluminescence system with ECL reagent from Thermo Scientific (catalog no. 1859023/185022).

Immunofluorescence. After respective treatments and at the indicated time points, primary hepatocytes plated on collagen-coated coverslips were treated with 75 nM LysoTracker Deep Red (Thermo Fisher Scientific, catalog no. L12492) for 15 min in the same medium. The cells were then rinsed once with phosphate-buffered saline (PBS) and fixed in chilled 4% paraformaldehyde (PFA) for 30 min. After fixation, the cells were washed three times with PBST (PBS with 0.1% Tween 20). After being blocked and permeabilized in 5% BSA and 0.5% Triton X in PBST for 40 min, the cells were incubated overnight at 4°C with mTOR antibody (Cell Signaling Technologies, catalog no. 2983). The cells were then incubated with Alexa Fluor 647-conjugated anti-rabbit antibody (Thermo Fisher Scientific, catalog no. L12492) for 1 h at room temperature, followed by washes in PBST. The coverslips were then mounted on a slide and imaged at $\times$40 using FluoView FV1200 laser scanning confocal microscope from Olympus Life Science. Three images per condition per experiment were analyzed for quantitation. The images were processed in ImageJ software by first converting into an 8-bit type, followed by thresholding at a constant value for all images, and the puncta per cell were counted using the "analyze particle" command. Negative-control images were processed similarly, and the values were subtracted from the test.

Oil red O staining. Primary hepatocytes plated in collagen-coated plates, after respective treatments, were rinsed once with PBS and fixed in chilled 4% PFA for 30 min. The cells were rinsed once again in PBS and freshly prepared and filtered Oil red O solution (40% in distilled water from a 0.5% stock solution in isopropanol) was added and kept for 15 min. The cells were washed in distilled water. The cells were then kept in water and imaged on an EVOS FLc microscope (Life Technologies, Inc.).

Antibodies. The following antibodies were used for Western blot analyses. Anti-phospho-S6K (Thr 389) (catalog no. 9234S), anti-p70-S6K (catalog no. 2708S), anti-phospho-ULK1 (Ser757; catalog no. 6888S), anti-ULK1 (catalog no. 8054S), anti-phospho-4E-BP1 (catalog no. 9456S), anti-4E-BP1 (catalog no. 9644S), anti-mTOR (catalog no. 2983), and anti-LC3A/B (catalog no. 12741S) were obtained from Cell Signaling Technologies (USA). Anti-β-actin (catalog no. A1978), anti-HA tag (catalog no. H6908; Sigma), anti-rabbit secondary (catalog no. A0545), and anti-mouse secondary (catalog no. A9044) antibodies were obtained from Sigma-Aldrich (USA).

RNA isolation and quantitation. Total RNA was extracted using the TRIzol reagent (catalog no. 15596018) according to the manufacturer's instructions. Then, 1 μg of RNA was reverse transcribed into cDNA using random hexamers and a SuperScript IV reverse transcriptase kit (catalog no. 18090200). PCR was carried out with KAPA SYBR FAST Universal 2$\times$ qPCR master mix (catalog no. KK4601)/LightCycler 480 SYBR green I Master kit (Roche catalog no. 14712220) in a Vapo.Protect Eppendorf LC-480 and LC-96 (Roche) system. The following primer pairs were used: human SIRT4, forward (5'-CAGCGCTTCATCACCC TTTC-3') and reverse (5'-CCTACGAAGTTTCTCGCCCA-3'); mouse SIRT4, forward (5'-ATCATCCCTGCAGGT GTACTCT-3') and reverse (5'-ATTAAAGGCAGCAACTCTCCACA-3'); human actin B, forward (5'-TGTACGT TGCTATCCAGGCTGT-3') and reverse (5'-TCTCCTTAATGTCACGCACGAT-3'); mouse actin B, forward (5'-G CATGGGTCAGAAGGATTCC-3') and reverse (5'-ACGCAGCTCATTGTAGAAGG-3'); mouse FASN, forward (5'-TTGCTGGCACTACAGAATG C-3') and reverse (5'-ACTCCCTGAATCATCAAAGG-3'); mouse SREBP1c, forward (5'-AACGTCACTTCCAGCTAGAC-3') and reverse (5'-GTAGAGGCTAAGCTGTCCCG-3'); mouse SCD1, forward (5'-CTGACCTGAAAGCCGAGAAG-3') and reverse (5'-AGAAGGTGCTAACGAACAGG-3'); and mouse CD36, forward (5'-GCGACATGATTAATGGCACAG-3') and reverse (5'-GATCCGAACACAGCGTAGAT AG-3').

α-Ketoglutarate assay and glutamate dehydrogenase assay. α-KG levels and GDH activity were assayed in cell lysates using α-KG measurement kit (catalog no. ab83431) and GDH activity kit (catalog no. ab102527) from Abcam according to the manufacturer's instructions. Briefly, the cells were lysed using the assay buffer provided in the kit and centrifuged at 13,000 rpm for 3 to 5 min at 4°C. For α-KG, the lysates were further deproteinized using perchloric acid and then processed according to the manufacturer's instructions. Both assays were set up in 96-well plates, and colorimetric readings were taken using a Tecan Infinite M200 Pro Plate reader system at 570 nm for α-KG and 450 nm for GDH. α-KG levels and the GDH activity were normalized to the protein concentration (estimated using a BCA kit [Pierce/Thermo-Fisher, catalog no. 23225]).

Luciferase assay. HepG2 cells were transfected with the luciferase expression construct under the FAS promoter (Addgene, catalog no. 8890) along with β-Gal plasmid (Ambion, catalog no. 5791). After 12 h of

transfection, the cells were transduced with either Ad-CMV or Ad-SIRT4 for another 24 h, and then the cells were kept for 6 h in either low (5 mM)- or high (25 mM)-glucose medium. The cells were harvested and lysed in passive lysis buffer (Promega, catalog no. E1941). A β-galactosidase assay was performed using ONPG (o-nitrophenyl-β-D-galactopyranoside; Sigma, catalog no. N1127) as a substrate. A luciferase assay was performed with the luciferase assay system (Promega, catalog no. E1500) according to the manufacturer's instructions. Luminescence counts were measured using an Infinite-M200-Pro (Tecan) or TriStarLB941 (Berthold technologies) and normalized to the β-galactosidase values to determine relative luciferase units.

Metabolite extractions and measurements by LC-MS/MS. Primary hepatocytes from wild-type and SIRT4KO were grown in high-glucose (25 mM) and glutamine (4 mM)-containing media for ~36 h. The cells were rapidly harvested, and metabolite was extracted as described earlier (53, 54). Briefly, cells in T-75 flasks were given an ice-cold 10% methanol wash, followed by scraping and collection in 1.5 ml of 80% methanol maintained at −45°C and vortexed for 15 s. The samples were incubated at −45°C for 15 min and then centrifuged at 14,000 rpm for 10 min at −5°C. Then, 1.4 ml of the supernatant was taken into a fresh tube and recentrifuged. The supernatant was distributed into several tubes and dried using a SpeedVac for 2 to 3 h. The samples were stored at −80°C. For TCA metabolites, the samples were derivatized using OBHA and EDC, followed by extraction in ethyl acetate. Metabolites were measured using LC-MS as described earlier (54, 55).

Cell proliferation assay. HEK293T cells transiently transfected with control and SIRT4-HA vectors were plated in equal cell densities. Cells were harvested at different time points of 12, 24, 36, 48, and 72 h by trypsinization and counted using a hemocytometer counting chamber by the trypan blue dye exclusion method. Cells were counted in triplicates for each set.

Data processing and statistical analysis. Western blot and immunofluorescence data were analyzed using ImageJ software. A Student t test and analysis of variance (ANOVA) were used for statistical analyses. Microsoft Excel was used for data processing, and the statistical significance was calculated using Excel or GraphPad Prism 5.0. The results are expressed as means ± the standard deviations (SD; or as indicated). All experiments were performed at least twice, with a minimum of three to six replicates.

REFERENCES

1. Efeyan A, Zoncu R, Sabatini DM. 2012. Amino acids and mTORC1: from lysosomes to disease. Trends Mol Med 18:524–533. https://doi.org/10.1016/j.molmed.2012.05.007.
2. Dibble CC, Manning BD. 2013. Signal integration by mTORC1 coordinates nutrient input with biosynthetic output. Nat Cell Biol 15:555–564. https://doi.org/10.1038/ncb2763.
3. Houtkooper RH, Pirinen E, Auwerx J. 2012. Sirtuins as regulators of metabolism and healthspan. Nat Rev Mol Cell Biol 13:225–238. https://doi.org/10.1038/nrm3293.
4. Haigis MC, Sinclair DA. 2010. Mammalian sirtuins: biological insights and disease relevance. Annu Rev Pathol 5:253–295. https://doi.org/10.1146/annurev.pathol.4.110807.092250.
5. Bheda P, Jing H, Wolberger C, Lin H. 2016. The substrate specificity of sirtuins. Annu Rev Biochem 85:405–429. https://doi.org/10.1146/annurev-biochem-060815-014537.
6. Price NL, Gomes AP, Ling AJ, Duarte FV, Martin-Montalvo A, North BJ, Agarwal B, Ye L, Ramadori G, Teodoro JS, Hubbard BP, Varela AT, Davis JG, Varamini B, Hafner A, Moaddel R, Rolo AP, Coppari R, Palmeira CM, de Cabo R, Baur JA, Sinclair DA. 2012. SIRT1 is required for AMPK activation and the beneficial effects of resveratrol on mitochondrial function. Cell Metab 15:675–690. https://doi.org/10.1016/j.cmet.2012.04.003.
7. Canto C, Jiang LQ, Deshmukh AS, Mataki C, Coste A, Lagouge M, Zierath JR, Auwerx J. 2010. Interdependence of AMPK and SIRT1 for metabolic adaptation to fasting and exercise in skeletal muscle. Cell Metab 11:213–219. https://doi.org/10.1016/j.cmet.2010.02.006.
8. Canto C, Gerhart-Hines Z, Feige JN, Lagouge M, Noriega L, Milne JC, Elliott PJ, Puigserver P, Auwerx J. 2009. AMPK regulates energy expenditure by modulating NAD$^+$ metabolism and SIRT1 activity. Nature 458:1056–1060. https://doi.org/10.1038/nature07813.
9. Ruderman NB, Xu XJ, Nelson L, Cacicedo JM, Saha AK, Lan F, Ido Y. 2010. AMPK and SIRT1: a long-standing partnership? Am J Physiol Endocrinol Metab 298:E751–E760. https://doi.org/10.1152/ajpendo.00745.2009.
10. Inoki K, Kim J, Guan KL. 2012. AMPK and mTOR in cellular energy homeostasis and drug targets. Annu Rev Pharmacol Toxicol 52:381–400. https://doi.org/10.1146/annurev-pharmtox-010611-134537.
11. Alers S, Loffler AS, Wesselborg S, Stork B. 2012. Role of AMPK-mTOR-Ulk1/2 in the regulation of autophagy: cross talk, shortcuts, and feedbacks. Mol Cell Biol 32:2–11. https://doi.org/10.1128/MCB.06159-11.
12. Ghosh HS, McBurney M, Robbins PD. 2010. SIRT1 negatively regulates

the mammalian target of rapamycin. PLoS One 5:e9199. https://doi.org/10.1371/journal.pone.0009199.

13. Igarashi M, Guarente L. 2016. mTORC1 and SIRT1 cooperate to foster expansion of gut adult stem cells during calorie restriction. Cell 166:436–450. https://doi.org/10.1016/j.cell.2016.05.044.

14. Hong S, Zhao B, Lombard DB, Fingar DC, Inoki K. 2014. Cross-talk between sirtuin and mammalian target of rapamycin complex 1 (mTORC1) signaling in the regulation of S6 kinase 1 (S6K1) phosphorylation. J Biol Chem 289:13132–13141. https://doi.org/10.1074/jbc.M113.520734.

15. Hensley CT, Wasti AT, DeBerardinis RJ. 2013. Glutamine and cancer: cell biology, physiology, and clinical opportunities. J Clin Invest 123:3678–3684. https://doi.org/10.1172/JCI69600.

16. Zhang J, Pavlova NN, Thompson CB. 2017. Cancer cell metabolism: the essential role of the nonessential amino acid, glutamine. EMBO J 36:1302–1315. https://doi.org/10.15252/embj.201696151.

17. Jewell JL, Kim YC, Russell RC, Yu FX, Park HW, Plouffe SW, Tagliabracci VS, Guan KL. 2015. Metabolism: differential regulation of mTORC1 by leucine and glutamine. Science 347:194–198. https://doi.org/10.1126/science.1259472.

18. Duran RV, Oppliger W, Robitaille AM, Heiserich L, Skendaj R, Gottlieb E, Hall MN. 2012. Glutaminolysis activates Rag-mTORC1 signaling. Mol Cell 47:349–358. https://doi.org/10.1016/j.molcel.2012.05.043.

19. Chin RM, Fu X, Pai MY, Vergnes L, Hwang H, Deng G, Diep S, Lomenick B, Meli VS, Monsalve GC, Hu E, Whelan SA, Wang JX, Jung G, Solis GM, Fazlollahi F, Kaweeteerawat C, Quach A, Nili M, Krall AS, Godwin HA, Chang HR, Faull KF, Guo F, Jiang M, Trauger SA, Saghatelian A, Braas D, Christofk HR, Clarke CF, Teitell MA, Petrascheck M, Reue K, Jung ME, Frand AR, Huang J. 2014. The metabolite alpha-ketoglutarate extends lifespan by inhibiting ATP synthase and TOR. Nature 510:397–401. https://doi.org/10.1038/nature13264.

20. Ho L, Titus AS, Banerjee KK, George S, Lin W, Deota S, Saha AK, Nakamura K, Gut P, Verdin E, Kolthur-Seetharam U. 2013. SIRT4 regulates ATP homeostasis and mediates a retrograde signaling via AMPK. Aging (Albany NY) 5:835–849. https://doi.org/10.18632/aging.100616.

21. Ahuja N, Schwer B, Carobbio S, Waltregny D, North BJ, Castronovo V, Maechler P, Verdin E. 2007. Regulation of insulin secretion by SIRT4, a mitochondrial ADP-ribosyltransferase. J Biol Chem 282:33583–33592. https://doi.org/10.1074/jbc.M705488200.

22. Haigis MC, Mostoslavsky R, Haigis KM, Fahie K, Christodoulou DC, Murphy AJ, Valenzuela DM, Yancopoulos GD, Karow M, Blander G, Wolberger C, Prolla TA, Weindruch R, Alt FW, Guarente L. 2006. SIRT4 inhibits glutamate dehydrogenase and opposes the effects of calorie restriction in pancreatic beta cells. Cell 126:941–954. https://doi.org/10.1016/j.cell.2006.06.057.

23. Feldman JL, Baeza J, Denu JM. 2013. Activation of the protein deacetylase SIRT6 by long-chain fatty acids and widespread deacylation by mammalian sirtuins. J Biol Chem 288:31350–31356. https://doi.org/10.1074/jbc.C113.511261.

24. Anderson KA, Huynh FK, Fisher-Wellman K, Stuart JD, Peterson BS, Douros JD, Wagner GR, Thompson JW, Madsen AS, Green MF, Sivley RM, Ilkayeva OR, Stevens RD, Backos DS, Capra JA, Olsen CA, Campbell JE, Muoio DM, Grimsrud PA, Hirschey MD. 2017. SIRT4 is a lysine deacylase that controls leucine metabolism and insulin secretion. Cell Metab 25:838–855.e815. https://doi.org/10.1016/j.cmet.2017.03.003.

25. Nasrin N, Wu X, Fortier E, Feng Y, Bare OC, Chen S, Ren X, Wu Z, Streeper RS, Bordone L. 2010. SIRT4 regulates fatty acid oxidation and mitochondrial gene expression in liver and muscle cells. J Biol Chem 285:31995–32002. https://doi.org/10.1074/jbc.M110.124164.

26. Komlos D, Mann KD, Zhuo Y, Ricupero CL, Hart RP, Liu AY, Firestein BL. 2013. Glutamate dehydrogenase 1 and SIRT4 regulate glial development. Glia 61:394–408. https://doi.org/10.1002/glia.22442.

27. Fernandez-Marcos PJ, Serrano M. 2013. Sirt4: the glutamine gatekeeper. Cancer Cell 23:427–428. https://doi.org/10.1016/j.ccr.2013.04.003.

28. Jeong SM, Xiao C, Finley LW, Lahusen T, Souza AL, Pierce K, Li YH, Wang X, Laurent G, German NJ, Xu X, Li C, Wang RH, Lee J, Csibi A, Cerione R, Blenis J, Clish CB, Kimmelman A, Deng CX, Haigis MC. 2013. SIRT4 has tumor-suppressive activity and regulates the cellular metabolic response to DNA damage by inhibiting mitochondrial glutamine metabolism. Cancer Cell 23:450–463. https://doi.org/10.1016/j.ccr.2013.02.024.

29. Csibi A, Fendt SM, Li C, Poulogiannis G, Choo AY, Chapski DJ, Jeong SM, Dempsey JM, Parkhitko A, Morrison T, Henske EP, Haigis MC, Cantley LC, Stephanopoulos G, Yu J, Blenis J. 2013. The mTORC1 pathway stimulates glutamine metabolism and cell proliferation by repressing SIRT4. Cell 153:840–854. https://doi.org/10.1016/j.cell.2013.04.023.

30. Nofal M, Zhang K, Han S, Rabinowitz JD. 2017. mTOR inhibition restores amino acid balance in cells dependent on catabolism of extracellular protein. Mol Cell 67:936–946.e935. https://doi.org/10.1016/j.molcel.2017.08.011.

31. Karaca M, Martin-Levilain J, Grimaldi M, Li L, Dizin E, Emre Y, Maechler P. 2018. Liver glutamate dehydrogenase controls whole-body energy partitioning through amino acid-derived gluconeogenesis and ammonia homeostasis. Diabetes 67:1949–1961. https://doi.org/10.2337/db17-1561.

32. Laurent G, German NJ, Saha AK, de Boer VC, Davies M, Koves TR, Dephoure N, Fischer F, Boanca G, Vaitheesvaran B, Lovitch SB, Sharpe AH, Kurland IJ, Steegborn C, Gygi SP, Muoio DM, Ruderman NB, Haigis MC. 2013. SIRT4 coordinates the balance between lipid synthesis and catabolism by repressing malonyl CoA decarboxylase. Mol Cell 50:686–698. https://doi.org/10.1016/j.molcel.2013.05.012.

33. Kang SA, Pacold ME, Cervantes CL, Lim D, Lou HJ, Ottina K, Gray NS, Turk BE, Yaffe MB, Sabatini DM. 2013. mTORC1 phosphorylation sites encode their sensitivity to starvation and rapamycin. Science 341:1236566. https://doi.org/10.1126/science.1236566.

34. Choo AY, Blenis J. 2009. Not all substrates are treated equally: implications for mTOR, rapamycin-resistance and cancer therapy. Cell Cycle 8:567–572. https://doi.org/10.4161/cc.8.4.7659.

35. Choo AY, Yoon SO, Kim SG, Roux PP, Blenis J. 2008. Rapamycin differentially inhibits S6Ks and 4E-BP1 to mediate cell-type-specific repression of mRNA translation. Proc Natl Acad Sci U S A 105:17414–17419. https://doi.org/10.1073/pnas.0809136105.

36. Zhu Y, Yan Y, Principe DR, Zou X, Vassilopoulos A, Gius D. 2014. SIRT3 and SIRT4 are mitochondrial tumor suppressor proteins that connect mitochondrial metabolism and carcinogenesis. Cancer Metab 2:15. https://doi.org/10.1186/2049-3002-2-15.

37. Shaw RJ. 2009. LKB1 and AMP-activated protein kinase control of mTOR signaling and growth. Acta Physiol (Oxf) 196:65–80. https://doi.org/10.1111/j.1748-1716.2009.01972.x.

38. Dennis PB, Jaeschke A, Saitoh M, Fowler B, Kozma SC, Thomas G. 2001. Mammalian TOR: a homeostatic ATP sensor. Science 294:1102–1105. https://doi.org/10.1126/science.1063518.

39. Gwinn DM, Shackelford DB, Egan DF, Mihaylova MM, Mery A, Vasquez DS, Turk BE, Shaw RJ. 2008. AMPK phosphorylation of raptor mediates a metabolic checkpoint. Mol Cell 30:214–226. https://doi.org/10.1016/j.molcel.2008.03.003.

40. Sabatini DM. 2017. Twenty-five years of mTOR: uncovering the link from nutrients to growth. Proc Natl Acad Sci U S A 114:11818–11825. https://doi.org/10.1073/pnas.1716173114.

41. Rogala KB, Gu X, Kedir JF, Abu-Remaileh M, Bianchi LF, Bottino AMS, Dueholm R, Niehaus A, Overwijn D, Fils AP, Zhou SX, Leary D, Laqtom NN, Brignole EJ, Sabatini DM. 2019. Structural basis for the docking of mTORC1 on the lysosomal surface. Science 366:468–475. https://doi.org/10.1126/science.aay0166.

42. Sancak Y, Bar-Peled L, Zoncu R, Markhard AL, Nada S, Sabatini DM. 2010. Ragulator-Rag complex targets mTORC1 to the lysosomal surface and is necessary for its activation by amino acids. Cell 141:290–303. https://doi.org/10.1016/j.cell.2010.02.024.

43. Horton JD, Goldstein JL, Brown MS. 2002. SREBPs: activators of the complete program of cholesterol and fatty acid synthesis in the liver. J Clin Invest 109:1125–1131. https://doi.org/10.1172/JCI15593.

44. Haspel J, Shaik RS, Ifedigbo E, Nakahira K, Dolinay T, Englert JA, Choi AM. 2011. Characterization of macroautophagic flux in vivo using a leupeptin-based assay. Autophagy 7:629–642. https://doi.org/10.4161/auto.7.6.15100.

45. Kim J, Kundu M, Viollet B, Guan KL. 2011. AMPK and mTOR regulate autophagy through direct phosphorylation of Ulk1. Nat Cell Biol 13:132–141. https://doi.org/10.1038/ncb2152.

46. Hindupur SK, Gonzalez A, Hall MN. 2015. The opposing actions of target of rapamycin and AMP-activated protein kinase in cell growth control. Cold Spring Harb Perspect Biol 7:a019141. https://doi.org/10.1101/cshperspect.a019141.

47. Parhofer KG. 2015. Interaction between glucose and lipid metabolism: more than diabetic dyslipidemia. Diabetes Metab J 39:353–362. https://doi.org/10.4093/dmj.2015.39.5.353.

48. Ding RB, Bao J, Deng CX. 2017. Emerging roles of SIRT1 in fatty liver diseases. Int J Biol Sci 13:852–867. https://doi.org/10.7150/ijbs.19370.

49. Tan Z, Luo X, Xiao L, Tang M, Bode AM, Dong Z, Cao Y. 2016. The role of

PGC1α in cancer metabolism and its therapeutic implications. Mol Cancer Ther 15:774–782. https://doi.org/10.1158/1535-7163.MCT-15-0621.

50. Khan SA, Sathyanarayan A, Mashek MT, Ong KT, Wollaston-Hayden EE, Mashek DG. 2015. ATGL-catalyzed lipolysis regulates SIRT1 to control PGC-1alpha/PPAR-α signaling. Diabetes 64:418–426. https://doi.org/10.2337/db14-0325.

51. Mukhopadhyay S, Frias MA, Chatterjee A, Yellen P, Foster DA. 2016. The enigma of rapamycin dosage. Mol Cancer Ther 15:347–353. https://doi.org/10.1158/1535-7163.MCT-15-0720.

52. Luo J, Deng ZL, Luo X, Tang N, Song WX, Chen J, Sharff KA, Luu HH, Haydon RC, Kinzler KW, Vogelstein B, He TC. 2007. A protocol for rapid generation of recombinant adenoviruses using the AdEasy system. Nat Protoc 2:1236–1247. https://doi.org/10.1038/nprot.2007.135.

53. Tu BP, Mohler RE, Liu JC, Dombek KM, Young ET, Synovec RE, McKnight SL. 2007. Cyclic changes in metabolic state during the life of a yeast cell. Proc Natl Acad Sci U S A 104:16886–16891. https://doi.org/10.1073/pnas.0708365104.

54. Walvekar A, Rashida Z, Maddali H, Laxman S. 2018. A versatile LC-MS/MS approach for comprehensive, quantitative analysis of central metabolic pathways. Wellcome Open Res 3:122. https://doi.org/10.12688/wellcomeopenres.14832.1.

55. Laxman S, Sutter BM, Shi L, Tu BP. 2014. Npr2 inhibits TORC1 to prevent inappropriate utilization of glutamine for biosynthesis of nitrogen-containing metabolites. Sci Signal 7:ra120. https://doi.org/10.1126/scisignal.2005948.